



Zircon U–Pb ages in El Chaltén Jurassic rhyolites (Chon Aike Silicic LIP, Argentina) reveal xenocrystic remnants of an unexposed lower basement of the Paleo-Pacific Gondwana margin

M.L. Foley^{*}, Z. Guillermin, B. Putlitz, L.P. Baumgartner

University of Lausanne, Geopolis, Mouline, 1015, Lausanne, Switzerland

ARTICLE INFO

Keywords:

Chon Aike silicic LIP
Zircon
Geochronology
Inheritance
Gondwana

ABSTRACT

We investigate the Jurassic volcanic rocks of the El Quemado Complex in the El Chaltén region (Argentina), which correlate with the youngest eruptive event of the Chon Aike Silicic LIP in southern Patagonia. New zircon crystallization ages of the various silicic units were obtained using U–Pb geochronology measured by in-situ Laser Ablation Inductively Coupled Plasma Mass Spectrometry. The average ages for 12 samples range from 147 to 152 Ma. Xenocrystic zircon cores of Jurassic igneous zircons are characterized by complex cathodoluminescent textures wherein growth surfaces are truncated by dissolution surfaces that are in turn overgrown by euhedral growth zones that exhibit oscillatory magmatic zoning. The cores have a wide range of ages, from 185 Ma to 1.3 Ga. We combine our analyzed xenocryst zircon ages preserved in the El Quemado Complex rhyolites with a compilation of published xenocryst zircon ages documented from Cenozoic to Paleozoic volcanic and plutonic rocks throughout southern Patagonia. The combined datasets suggests three prominent geologic features not currently exposed on the present day surface: (1) widespread abundant Triassic through Permian (200–300 Ma) xenocrystic ages throughout the present day Andean region, which connect to current exposures in Northern Patagonian and that of the Antarctic Peninsula, marking the Paleo-Pacific Gondwanan margin, (2) the existence of widespread Early-Middle Ordovician to Cambrian ages throughout southern Patagonia, and (3) the presence of an old (~1.0 Ga) crust below that of the Deseado Massif and Tierra del Fuego, which likely extends beneath the present-day Andes.

1. Introduction

Geochronological studies of inherited igneous zircon highlight the complex nature of crustal reservoirs involved in magma genesis (Miller et al., 1992, 2007; Bryan et al., 2008; Farina et al., 2018). *In situ* analysis of zircon can provide invaluable information on both the timing of new zircon crystallization in a melt by analyzing overgrowth zones that formed in the hosting melt and on the antecedent history of assimilated crust by analyzing xenocrystic zircon cores. Zircon is a common accessory mineral in silicic magmas and its refractory behavior allows for monitoring crustal development and modification throughout Earth's history (Condie et al., 2009; Claiborne et al., 2010; Miller et al., 2011; Carley et al., 2011; Bindeman and Melnik, 2016). In combination, silicic magmas have the potential to sample the deep crust via melting and/or assimilation (Miller et al., 1988; Clemens et al., 2021; Jacob et al., 2021), therefore providing insight into portions of the crustal section

which may not be exposed at the surface. Zircon xenocrysts are often interpreted as the surviving remnants of partially melted older crustal material, and therefore these zircons may serve as to fingerprint anatectic source components for their new host magmas. Throughout this study, we distinguish zircon populations as either *xenocrystic*, inherited grains derived from a contributing source material and/or entrained via assimilation related contamination, or as *magmatic*, which are directly precipitated from the host melt (Miller et al., 2003, 2007).

The nature of the continental crust in southern Patagonian is under discussion, with long-standing debates about its origin and relationship with the South American continent (Forsythe, 1982; Pankhurst et al., 2003, 2006; Ramos, 2008; Ramos and Naipauer, 2014; Calderón et al., 2016; Suárez et al., 2019a; Rojo et al., 2021a). The timing of mantle melt extraction events can be estimated with xenolith bulk-rock radiogenic isotopic systematics (e.g., Sm–Nd or ReOs; Pankhurst and Rapela, 1995; Schilling et al., 2017). However, insights into geologically significant

^{*} Corresponding author.

E-mail address: michelle.foley@unil.ch (M.L. Foley).

<https://doi.org/10.1016/j.jsames.2021.103690>

Received 15 September 2021; Received in revised form 2 December 2021; Accepted 17 December 2021

Available online 21 December 2021

0895-9811/© 2021 The Authors. Published by Elsevier Ltd. This is an open access article under the CC BY license (<http://creativecommons.org/licenses/by/4.0/>).

events that resulted in the growth of new crust in the past related to intermediate to silicic magmatism are limited, unless currently exposed at the surface. Lower-crustal xenocrysts or xenoliths incorporated into igneous bodies prior to magma ascension provide indirect sampling of the crustal column. While some studies use xenoliths to decipher the age and composition of the upper-mantle to lower-crustal region in Patagonia (e.g., Pankhurst and Rapela, 1995; Schilling et al., 2017), relatively few studies use xenocrystic zircon in southern Patagonia (e.g., Rolando et al., 2002; Orihashi et al., 2013).

The main physiographic features of Patagonia are separated into the Andean Cordilleran along the western margin of South America and into the extra-Andean region in the east. The extra-Andean region of Patagonia comprises two stable crystalline blocks, including the North Patagonian Massif (or Somun Cura Massif) and the Deseado Massif (Fig. 1a); both massifs contain the oldest known crystalline basements in Patagonia (Harrington, 1962; Pankhurst et al., 2003, 2006, 2014; Ramos, 2008). Largely obscured by later tectonic events associated with the convergent Andean margin, a major missing link that remains in our current understanding is the connection between the lower crustal basement(s) which comprise the Deseado Massif region and that of the southern Patagonian Andes. Here we provide new evidence for (1) the possible ages of the underlying crust around the Precordillerian area of the southern Andean region and (2) a possible tectonic link to the crystalline basements of the Deseado Massif and Tierra del Fuego regions.

We present new laser ablation inductively coupled mass spectrometry (LA-ICP-MS) U–Pb ages for both magmatic and xenocrystic zircons from multiple eruptive units (n = 16 samples) of the El Quemado

Complex (EQC) within the region of El Chaltén (Argentina). The silicic volcanic rocks of the EQC studied in El Chaltén presents a special case for the study of xenocrystic zircon, because they reflect crustal derived magmas generated during widespread crustal anatexis based on oxygen isotope analysis (Seitz et al., 2018). We combine our analyzed zircon xenocryst ages preserved in the El Quemado Complex rhyolites with a compilation of published zircon xenocryst ages documented from Cenozoic to Paleozoic volcanic and plutonic rocks throughout southern Patagonia. Using the combined datasets, we explore the prospect of older, unexposed igneous basement(s) underlying the Magallanes (Austral) Basin, and below the Andes around latitudes ~48°–51° S (Fig. 1a).

2. Geological background

The Chon Aike Silicic LIP (CASP) covers an area of ~1 million km² throughout the southern Patagonian region and partially the Antarctic Peninsula (Fig. 1a; Pankhurst and Rapela, 1995; Pankhurst et al., 1998). Basement outcrops are limited due to extended ice cover in the western Andes and near-complete cover of the basement due to its burial from the extensive volcanism of the Jurassic CASP to the east. Deformation related to the Andean orogeny and subsequent intrusion of the Patagonian Batholith have dissected potential basement blocks, further complicating the interpretation of the basement.

The oldest exposed units of the southern Patagonian Andes comprise the pre-rift Carboniferous-Devonian Gondwanan metasedimentary basement of the Eastern Andean Metamorphic Complex (EAMC) (Hervé et al., 2003, 2008; Augustsson et al., 2006; Giacosa et al., 2012a). The

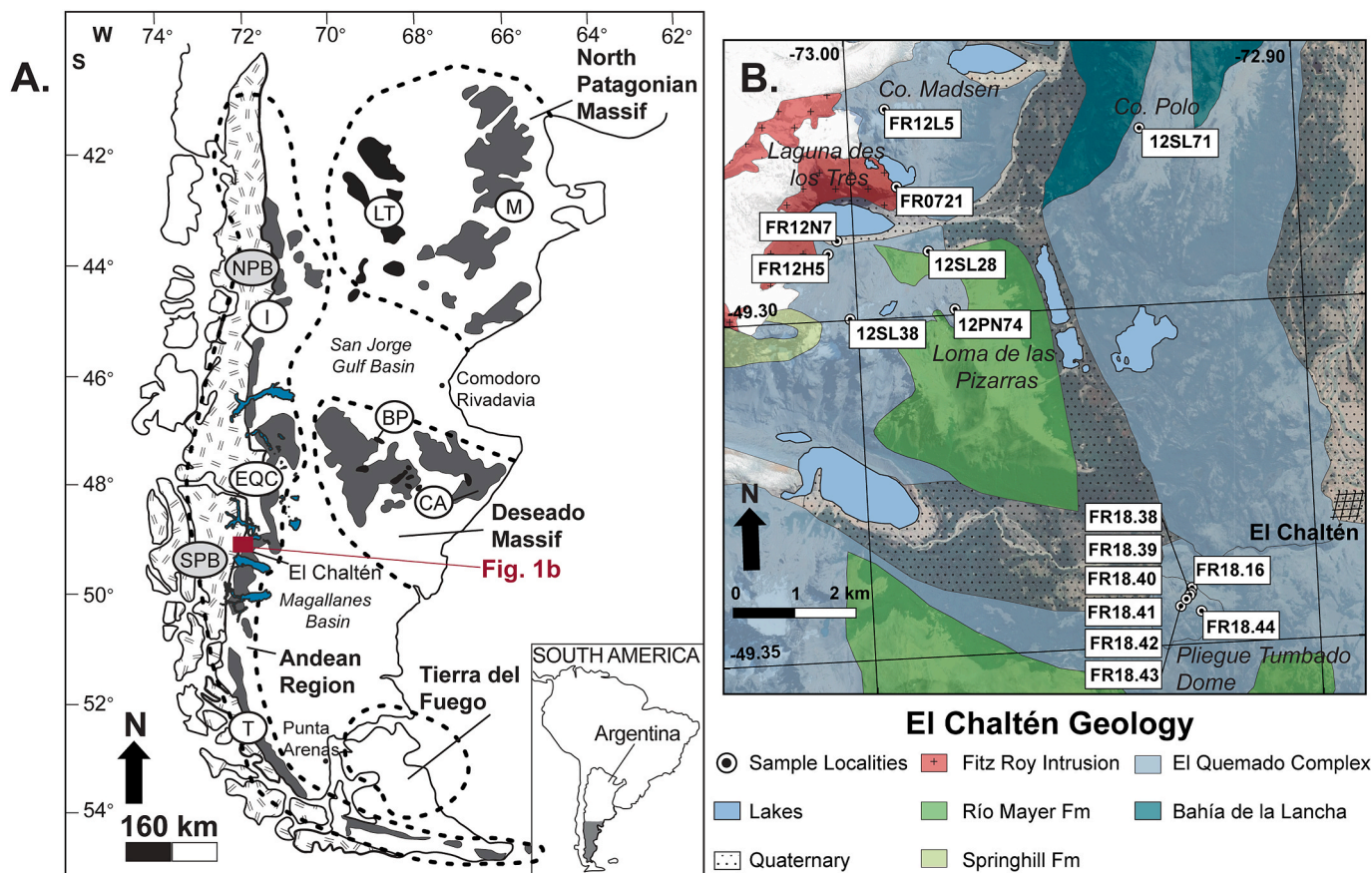


Fig. 1. (A) Simplified geologic map of Patagonia showing the extent of the Chon Aike Silicic LIP (dark grey and black), the northern (NPB) and southern Patagonia Batholith (SPB) as indicated by the hatched pattern, and the four major geological regions. The formations of the Chon Aike Silicic LIP include: the Marifil Formation (M), the Lonco Trapial Formation (LT), the Bajo Pobre Formation (BP), the Chon Aike Formation (CA), the Ibañez Formation (I), the El Quemado Complex (EQC), and the Tobifería Formation (T). (B) Simplified geologic map of the El Chaltén region with sample locations shown (modified from Giacosa et al., 2012b and Seitz et al., 2018).

EAMC has been assigned multiple formation names, depending on its location in the Andes. In the south, basement rocks of the EAMC are defined as the Bahía de la Lancha (Argentina-Chile) and Cochrane (Chile) formations and are mostly made up of alternating greywackes and pelites (Riccardi, 1971). To the north, the low-grade EAMC rocks are classified as Río Lacteo (Argentina) and Lago General Carrera (Chile) formations (Riccardi, 1971; Leanza, 1972). In general, the EAMC is comprised of low-grade, quartz-rich, turbidite protolith metasedimentary units. In El Chaltén, the complex is a succession of phyllites, metagraywackes and metasandstones (Giacosa et al., 2012a).

Recently described outside of the Chaltén area are the metamorphic rocks of the Nunatak Viedma unit (Suárez et al., 2019b). Originally, this unit was assigned to the Bahía de la Lancha formation (EAMC) by the Argentine Geological-Mining Survey based on proximity and lithological similarities (e.g., Giacosa et al., 2012b). This unit has a maximum depositional age of ~220 Ma (average of three metapsammite samples: 225, 223, and 212 Ma; Suárez et al., 2019b), therefore these Triassic ages clearly defines it as a different tectonostratigraphic unit within the pre-Andean metamorphic belt. Similar to the EAMC, the metamorphic conditions are estimated to have only reached sub-greenschist to greenschist facies.

In much of the eastern southern Patagonian Andes, the Bahía de la Lancha is uncomfortably overlain by late Jurassic volcanic units. These rocks together are locally faulted, tilted, and thrust due to the Andean deformation (e.g., Ramos, 1989; Giacosa et al., 2012a; Ghiglione et al., 2019). The Jurassic volcanic rocks along the Andean margin make up the El Quemado Complex, which marks the youngest eruptive episode of the Chon Aike Silicic LIP (Pankhurst et al., 2000; Poblete et al., 2013; Malkowski et al., 2016). The CASP extends throughout much of southern Patagonia and into the Antarctic Peninsula, with an estimated eruptive volume of ~230,000 km³ (Fig. 1a) (Pankhurst et al., 1998). The province is predominately silicic, with volumetrically ~90% of the erupted material is estimated to have >70 wt % SiO₂, with minor volumes of andesite and dacite present (Gust et al., 1985; Riley et al., 2001). Most of the CASP volcanic rocks were emplaced during a period of major extension associated with the breakup of Gondwana; geochemistry of the youngest EQC units indicates an increasingly important role of subduction-zone magmatism along the Paleo-Pacific margin (Riley et al., 2001; Rapela et al., 2005).

Current known U–Pb zircon crystallization ages of the CASP range from ca. 146 Ma to 192 Ma (Poblete et al., 2013; Pavón Pivetta et al., 2019). The onset of CASP magmatism started in the North Patagonian Massif (NPM) (Fig. 1a) at ca. 192 Ma with the silicic Marifil Formation (eastern NPM) and andesitic Lonco Trapial Formation (western NPM) progressing until ca. 178 Ma. Afterwards, CASP magmatism progressed southward into the eastern Deseado Massif with the eruption of the silicic Chon Aike Formation and andesitic Bajo Pobre Formation ranging from 167 to 179 Ma (Pankhurst et al., 2000; Navarrete et al., 2020). The last eruptive phase of the CASP includes the continuation of the Chon Aike Formation in the western Deseado Massif at ca. 160 Ma (Dube et al., 2003; Lopez, 2006; Moreira et al., 2009; Permuy-Vidal et al., 2021; Foley et al., 2021) and the youngest formations at ca. 150 Ma erupted along the Andean margin, including the El Quemado Complex (EQC) and its equivalent formations in Chile, the Ibañez (Baker et al., 1981) and Tobífera Formations. Ages for the EQC and Ibañez Formation are reported between 146 and 157 Ma (Pankhurst et al., 2000; Rolando et al., 2004; Poblete et al., 2013; Malkowski et al., 2016; Foley et al., 2021). The earliest age determined for the Tobífera Formation was 171.8 ± 1.2 Ma from a borehole sample at a depth of 2518 m (Pankhurst et al., 2000). However, a more recently determined SHRIMP U–Pb age of ca. 149 Ma was reported, closer to those ages of the EQC near 51°30'S (Calderón et al., 2004; Calderón, 2006; Calderón et al., 2007), while at a latitude of 52°, a weighted mean SHRIMP U–Pb age of 159.9 ± 1.1 Ma was reported for a mylonitic silicic metatuff of the Tobífera Formation (Muller et al., 2021).

3. Methods

Sixteen samples of volcanic rocks of different eruptive units were crushed and sieved at grain sizes of 250–125 µm, 125–90 µm, and <90 µm grain. Zircons were separated from the different size fractions after a series of panning, Frantz magnetic separator, and heavy liquids (methylene iodide) treatment. Zircon grains were mounted in 25 mm EpoFix epoxy discs and polished to expose the grain interiors. Zircons were imaged on a scanning electron microscope (SEM) with cathodoluminescence (CL) to image their interior textures, using the CL detector attached to the JEOL JXA-8350F FEIG-electron microprobe or the CamScan MV2300 SEM (W filament source) at the University of Lausanne. CL images were acquired with an accelerating voltage of ~10 kV on the microprobe and 15 kV on the SEM; images acquired with the SEM require a higher kV (15 kV) due to the lower-resolution filament source. CL images were used to characterize internal structures and to target areas of interest for age analyses.

U–Pb ages were measured on the polished zircon surfaces using a LA-ICP-MS on an Agilent 7700 quadrupole spectrometer coupled with a GeoLas 200M ArF ablation system at the University of Lausanne. Individual measurements were performed with a repetition rate of 5HZ, an energy density on the sample of 3 J/cm² and a spot size of 30 µm, using helium as the carrier gas. For samples that yielded abundant zircon, we selected ~20 representative grains to analyze; for samples with less zircon, we analyzed all separated grains. We used the GEMOC GJ-1 zircon (Chemical Abrasion-Isotope Dilution-Thermal Ionization Mass Spectrometry) ²⁰⁶Pb/²³⁸U age of 600.5 ± 0.4 Ma; Horstwood et al., 2016) as the primary standard during analysis to monitor data precision and accuracy throughout analysis. The Plešovice natural reference zircon (337.207 ± 0.029 Ma; Sláma et al., 2008; Widmann et al., 2019) was used as the secondary standard to normalize isotopic fractionation during analysis. Data reduction was carried out using LAMTRACE (Jackson, 2008). Analyses were only considered concordant if the error ellipse overlaps with Concordia (including the width of uncertainty associated with the calculation of the uranium decay equation); only concordant analyses are included in the calculation of sample weighted mean ages. Concordia diagrams (2σ error ellipses), intercept ages, and weighed mean ages were calculated using the Isoplot/Ex software (Ludwig, 2003). Samples which have very small number of concordant analysis are not considered representative the average crystallization age of the sample.

4. Sample localities and rock descriptions

The study area is located within Los Glaciares National Park in Argentina, bordering the town of El Chaltén, more widely known for the Miocene composite intrusion of Fitz Roy (Ramírez de Arellano et al., 2012). We collected multiple rhyolitic samples from localities to the west of El Chaltén (Fig. 1b). The easternmost samples were collected from two locations which show very minor Andean deformation, and no visible metamorphic overprint. These are the sample localities south of Cerro Polo and a rhyolite dome on the south slope of the Río Fitz Roy (Fig. 1b). The western samples were collected within the strongly folded and faulted Andean front, between the Loma de las Pizarras and the Co. Madsen peaks (Figs. 1b and 2a). The samples have seen regional anchizonal metamorphism. Samples close to the Fitz Roy composite intrusions have undergone additional contact metamorphism (Leresche, 2013).

Seitz et al. (2018) and Guillermin (2019) present whole rock geochemical data for most samples included in this study: FR12L5, FR0721, FR12N7, 12PN74, FR18.16, FR18.38, FR18.39, FR18.40, FR18.41, FR18.42, FR18.43, and FR18.44. Bulk silica contents range from lowermost 65 to uppermost 83 wt % SiO₂, with the majority of the units rhyolitic in composition (>70 wt % SiO₂). The phenocryst contents range from ~4 to 10%, including primary quartz, feldspar and biotite phenocrysts and accessories of zircon, apatite, and ilmenite. In all

samples, the matrix is devitrified and contains recrystallized aphanitic quartz and feldspar. The original phenocryst assemblages are estimated using the chemistry of the secondary mineral replacement and the pseudomorphs in thin sections.

Eastern samples: Samples were collected on the western cliff of the north ridge of the Co. Polo. Sample 12SL71 is from a tuff layer above the Bahía de la Lancha basement contact.

The Pliegue Tumbado dome is located on the southern slopes of the Río Fitz Roy, ca. 3.5 km east of El Chaltén). It forms the ridge below the Loma del Pliegue Tumbado lookout (Fig. 1b). The dome is elongated at least 1 km in the N–S direction and is roughly 300 m high. The central portion of the dome is predominantly composed of well-preserved, flow-banded rhyolites. In the external parts of the dome, rhyolite flows grade into heavily brecciated flows. No deformation features associated with the Andean orogeny are apparent close to the dome; hence, the succession of lava flows, breccia and ignimbrites is believed to represent the original structure of the dome upon emplacement. At least one synvolcanic normal fault is recognized in the frontal part of the Pliegue Tumbado Dome. Samples FR18.16 to FR18.44 were collected on the eastern flank of the dome. Samples with higher sample numbers are from successively higher – e.g., younger – flows (Fig. 2b).

Both the ignimbrite section of Co. Polo and the Pliegue Tumbado dome experienced moderate to strong hydrothermal alteration in which nearly all primary mafic minerals were altered to chlorite. Some samples show abundant calcite replacing feldspar phenocrysts. Calcite is also found in veins and in small aggregates in the matrix. Relict mafic minerals are biotite and rarely amphibole. Besides the hydrothermal alteration, these samples show no other deformation or metamorphism. The main alteration phases in the matrix are sericite, chlorite, and epidote. The temperatures of hydrothermal alteration are estimated to be ~200–300 °C according to the alteration assemblages (Guillermin, 2019). Volcaniclastic rocks and lava flows in the area have relict magmatic flow bands and vesicles.

Western samples: These samples were collected within the intensely folded front of the Andean Orogen. Here, the Andean regional metamorphism reached anchizonal conditions (Nescher, 2013). We distinguish two subgroups of samples: those which have only undergone regional metamorphism (Loma de las Pizarras), and the samples which have additionally experienced contact metamorphism due to the Fitz Roy intrusions (Laguna Sucia and Co. Madsen).

Three samples from the EQC were collected from different localities on the northern slopes of the Loma de las Pizarras. Sample 12SL28 is from the top of a rhyolite dome, at the base of the slope, samples 12PN74 and 12SL38 are from within the series (Fig. 2a). These samples have a fine-grained silicified matrix, often miarolitic cavities, and some flow banding. Calcite and/or chlorite alteration destroyed most mafic minerals and partially replaced feldspar. A slight schistosity is visible in quartz phenocrysts, along with undulose extinction.

Several samples were collected within the contact aureole. Samples FR12H5, and FR12N7 were collected within ca. 150 m of the contact with the tonalites of the Fitz Roy igneous complex at the south side of Laguna Sucia. Samples FR12H5 and FR12N7 show quartz phenocrysts deformed to oval, elongated quartz eyes. Contact metamorphic minerals can include biotite and some garnet and pinnitized cordierite. In the field, partial melting is suggested by pegmatoidal garnet bearing leucogranite. Sample FR0721 is a protomylonite collected just west of Laguna de los Tres at the contact with a gabbro within the Fitz Roy Complex. It shows textures similar to those of the samples above and has strongly deformed quartz phenocrysts, metamorphic white mica, and biotite. The last sample, FR12L5, is a slightly contact metamorphosed rhyolite with minor deformation, collected on the summit of Co. Madsen about 800 m from the intrusive contact with the gabbro of the Fitz Roy Plutonic Complex (Fig. 2a).

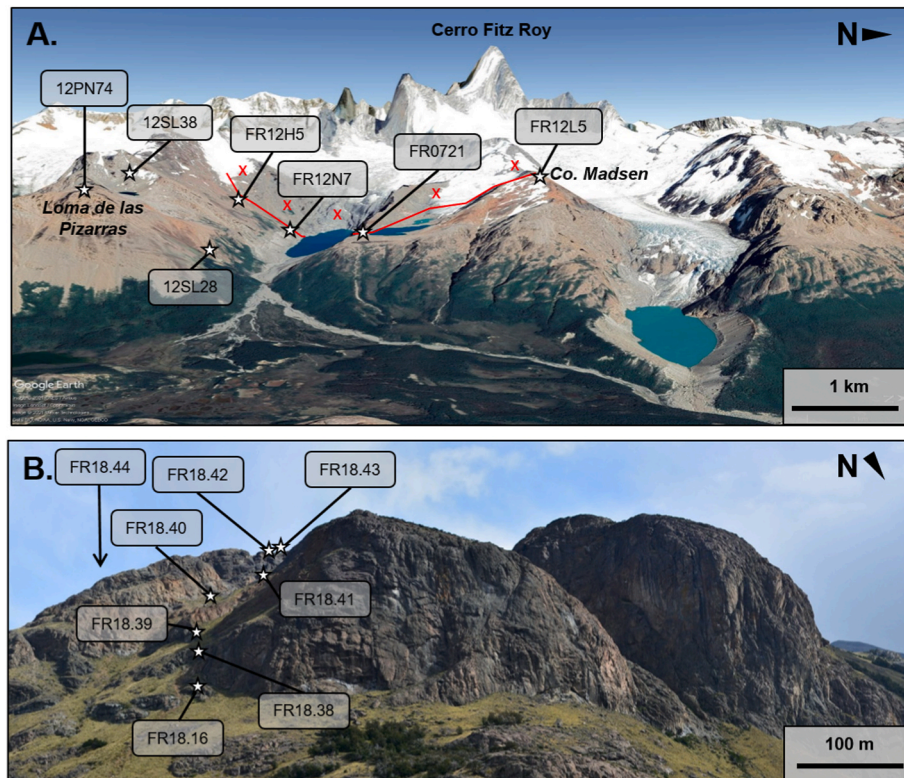


Fig. 2. Sampled units of the EQC in the El Chaltén region. (A) Google Earth imagery of rhyolite outcrops, east of Cerro Fitz Roy (indicated by red crosses), with sample localities (star) and location of the intrusion contact (red line); (B) Sample profile along the Pliegue Tumbado Dome; location of FR18.44 is not visible within this view of the dome.

5. CL imaging and LA-ICP-MS U–Pb results

Under the binocular, handpicked zircon is often pink to lilac and is typically euhedral to subeuhedral. SEM-CL imaging of most grains shows fine-scale oscillatory magmatic zoning; sector zoning is observed in some grains (Fig. 3).

The rhyolitic domes and the ignimbrite of Co. Polo a have a total range of concordant $^{206}\text{Pb}/^{238}\text{U}$ ages that span from ~140 to 159 Ma with average $^{206}\text{Pb}/^{238}\text{U}$ ages ranging from ~147 to 152 Ma (Fig. 4). A summary of total analyses per sample, the number of analyses (n) used to calculate an average age, and the corresponding mean squared weighted distribution MSWD per sample is recorded in Table 1. A table of all the analyses with the calculated percentage of discordance can be found in the supplementary material.

Many samples have a low number of concordant analysis per total number of spot analyses per sample (Supplementary). Combining 267 spot analyses for all 16 samples analyzed, roughly 50%, (138 analysis) were concordant, giving a total of ~50% of concordant measurements.

5.1. Magmatic ages from eastern EQC samples

Zircon U–Pb crystallization weighted mean ages range from ~147 to 151 Ma for a total of five samples from the Pliegue Tumbado dome (FR18.38, FR18.39, FR18.40 and FR18.43, FR18.44) (Figs. 4a and 5) (Table 1). The three samples with 10 or more concordant analyses have very similar average ages with two ages within error at 147.7 ± 1 Ma and 147.4 ± 1 Ma. The third is slightly older at 149.3 ± 1 Ma. The three remaining samples (FR18.16, FR18.41, and FR18.42) have a generally smaller number of concordant ages per sample (<3 analysis), but still record similar U–Pb ages ranging from 147.5 ± 1 Ma to 153.0 ± 3 Ma. No trend with stratigraphic collection horizon is evident.

A sample from the lowermost Cerro Polo section (12SL71), which directly overlies the metasedimentary basement of the Bahía de la Lancha Formation, was analyzed for zircon U–Pb. The ignimbrite has four concordant ages, from a total of 16 analysis. This sample provided a weighted mean $^{206}\text{Pb}/^{238}\text{U}$ age of 152.4 ± 2 Ma, which is calculated from three of the analyses (Fig. 4b).

5.2. Magmatic ages from western EQC samples

Three samples were taken from different rhyolites within the intensely folded Andean belt of the Loma de las Pizarras (Fig. 2a). Samples that lie outside of the contact aureole of the Fitz Roy igneous complex (12SL28, 12PN74, 12SL38; Figs. 1b and 2a) yield concordant ages of ~146–156 Ma. They are comparable to the ages obtained in the Eastern, minor-deformed Andean foreland. Due to the complexity of folding and faulting related to Andean deformation, it is difficult to discern contact relationships between individual rhyolitic domes. Nevertheless, based on structural reconstruction, we interpret that the samples are from three different but adjacent domes. Sample 12PN74 is towards the base of a dome, sample 12SL38 is within the middle of a dome, while sample 12SL28 was collected on top of a rhyolite dome. In total, three ages were calculated from these three samples which range from 146.9 ± 4 Ma (12SL28) to 151.2 ± 2 Ma (12SL38) (Fig. 4b and Supplementary).

Four samples were collected within the contact aureole of the Fitz Roy igneous complex. All four samples yield ages of 150–151 Ma, comparable to those of the others, even though they experienced high-grade contact metamorphism and significant deformation. The sample of Laguna de los Tres (FR021) yield a weighted mean $^{206}\text{Pb}/^{238}\text{U}$ age of 150.8 ± 1 Ma from 13 analyses concordant analysis, giving a MSWD of 2.4 (Supplementary). An anomalously young age was obtained at 117 ± 8 Ma (Fig. 5d).

5.3. El Chaltén area xenocrystic zircon cores

In addition to the Late Jurassic zircon crystallization ages, xenocrystic zircons with ages ranging from Middle Jurassic to Mesoproterozoic were analyzed within the Pliegue Tumbado Dome (eight samples) and in the rhyolite at Loma de las Pizarras (12PN74, Fig. 5C). The most obvious indication for the presence of xenocrystic cores is a distinctive change in CL intensity or pattern from core to rim (Fig. 6). Three of the cores have pronounced dissolution textures that separate the older core from the younger magmatic overgrowth. In other cases, the growth from the core to the rim appears less obvious and uninterrupted, even where there are abrupt changes in age (the 460–470 Ma

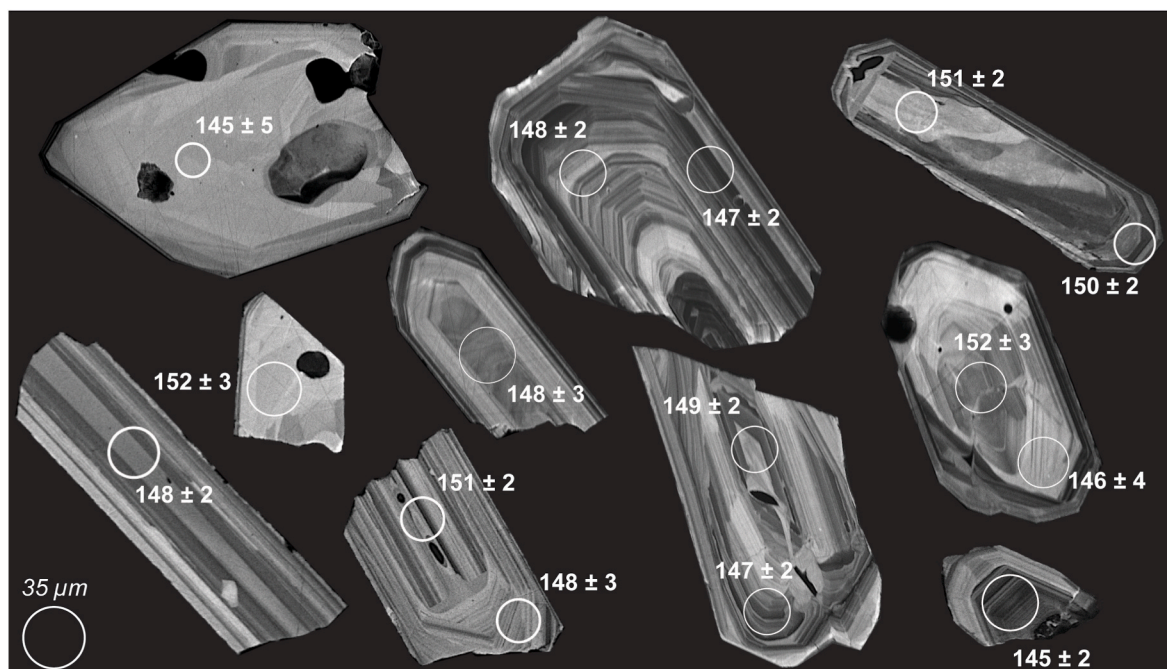


Fig. 3. Characteristic cathodoluminescent images of the Jurassic-aged magmatic zircon in the EQC silic volcanic units. Size of crystals are indicated by the LA-ICP-MS spot size (35 μm). All analyses depicted are concordant.

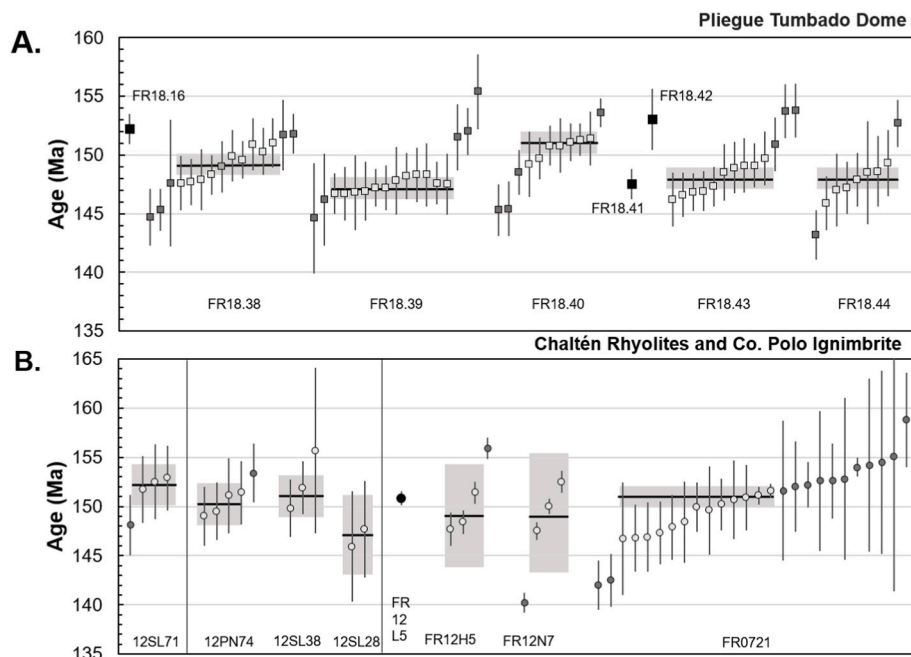


Fig. 4. Summary of Jurassic concordant analyses for all El Quemado Complex units measured during this study. (A) Pliegue Tumbado Dome and (B) six El Chaltén rhyolites and the basal Co. Polo ignimbrite; separated based on their location described in text. Black bar represents average age of each unit with corresponding error (grey bar). Samples which have too few of analysis to calculate an average age are represented by a single, black analysis. The darkened analysis (dark grey) within each sample indicates analyses excluded from the weighted average age.

Table 1
El Chaltén volcanic zircon U–Pb magmatic and inheritance ages by sample.

Sample	Locality	Latitude	Longitude	MSWD	Magmatic Crystallization $^{206}\text{Pb}/^{238}\text{U}$ Age (Ma)	Inheritance $^{206}\text{Pb}/^{238}\text{U}$ Age (Ma)
12PN74	Loma de las Pizarras	−49.29843	−72.98443	0.6	150 ± 2	185 ± 4
12SL38	Loma de las Pizarras	−49.29910	−73.00045	1.2	151 ± 2	
12SL28	Loma de las Pizarras	−49.28942	−72.97955	0.2	147 ± 4	
FR12L5	Cerro Madsen	−49.26892	−72.99134	NA	151 ± 1	
FR12H5	Laguna Sucia (at contact)	−49.29282	−73.00857	10	150 ± 5	
FR12N7	Laguna Sucia	−49.28875	−73.00503	25	150 ± 6	
FR0721	Laguna des los Tres	−49.28033	−72.99053	2.4	151 ± 1	
12SL71	Cerro Polo	−49.27632	−72.93695	0.1	152 ± 2	
FR18.16	Pliegue Tumbado Dome	−49.34176	−72.92830	NA	152 ± 2	281 ± 4
FR18.38	Pliegue Tumbado Dome	−49.34250	−72.92853	1.5	149 ± 1	166 ± 3; 169 ± 2; 206 ± 2
FR18.39	Pliegue Tumbado Dome	−49.34281	−72.92886	0.3	147 ± 1	
FR18.40	Pliegue Tumbado Dome	−49.34337	−72.92901	0.6	151 ± 1	
FR18.41	Pliegue Tumbado Dome	−49.16568	−73.19471	NA	148 ± 1	264 ± 2; 267 ± 2
FR18.42	Pliegue Tumbado Dome	−49.34438	−72.93102	NA	153 ± 3	1303 ± 13
FR18.43	Pliegue Tumbado Dome	−49.34438	−72.93102	1.5	148 ± 1	296 ± 4; 463 ± 7; 476 ± 4
FR18.44	Pliegue Tumbado Dome	−49.34524	−72.92643	0.8	148 ± 1	177 ± 6

core with a 154 Ma rim). Only some of the cores appear to be significantly rounded (Fig. 6).

Ten zircon grains with xenocrystic cores were analyzed from the seven samples of the Pliegue Tumbado Dome (Table 1). Of 20 spot analyses, 12 were concordant and have a wide range in $^{206}\text{Pb}/^{238}\text{U}$ age: 166 ± 3, 169 ± 2, 177 ± 6, 185 ± 4, 206 ± 2, 264 ± 2, 267 ± 2, 281 ± 4, 296 ± 4, 463 ± 7, 476 ± 4, and 1303 ± 13 Ma.

The span of inherited ages ranges from Late Jurassic to Mesoproterozoic. All inherited zircons appear with magmatic overgrowths, and all but one rim have overgrowths of Jurassic age (Fig. 6). In circumstances where rims are not analyzed, CL images reveal magmatic oscillatory overgrowths. Almost all inherited cores analyzed have CL patterns that represent magmatic growth. Only one single grain has a core which shows a CL texture that lacks the typical magmatic oscillatory zones. This core has two distinctive zones which are homogeneous in CL; both zones within this single grain preserve the oldest age in this study at 1.0 and 1.3 Ga, though the 1.0 Ga is slightly off Concordia (Supplementary).

6. Discussion

We present the first extensive dataset for LA-ICP-MS zircon U–Pb crystallization ages for multiple eruptive units in the El Chaltén area. Here, we compare our determined ages with those previously reported for the EQC, on a larger regional scale. We also discuss the significance of inherited ages measured in the Pliegue Tumbado Dome, which are combined with several additional igneous units of southern Patagonia to help characterize the unexposed lower crust and basement.

6.1. Jurassic magmatic ages from the Chaltén region

Our new data suggest that the CASP volcanism in the El Chaltén area occurred over a narrow time range of 147–154 Ma, with most of the zircon crystallization ages occurring between 148 and 152 Ma. This is consistent with ages reported by Malkowski et al. (2016) for the rhyolitic and submarine volcanic deposits of the Cerro Polo section (ca. 148 to 152 Ma). In both studies, the lowermost ignimbrite overlying the Bahía de la Lancha is dated at 152 Ma. These data continue to establish the EQC as the final volcanic episode of the Jurassic Chon Aike Silicic LIP (Pankhurst and Rapela, 1995; Pankhurst et al., 1998; Riley et al.,

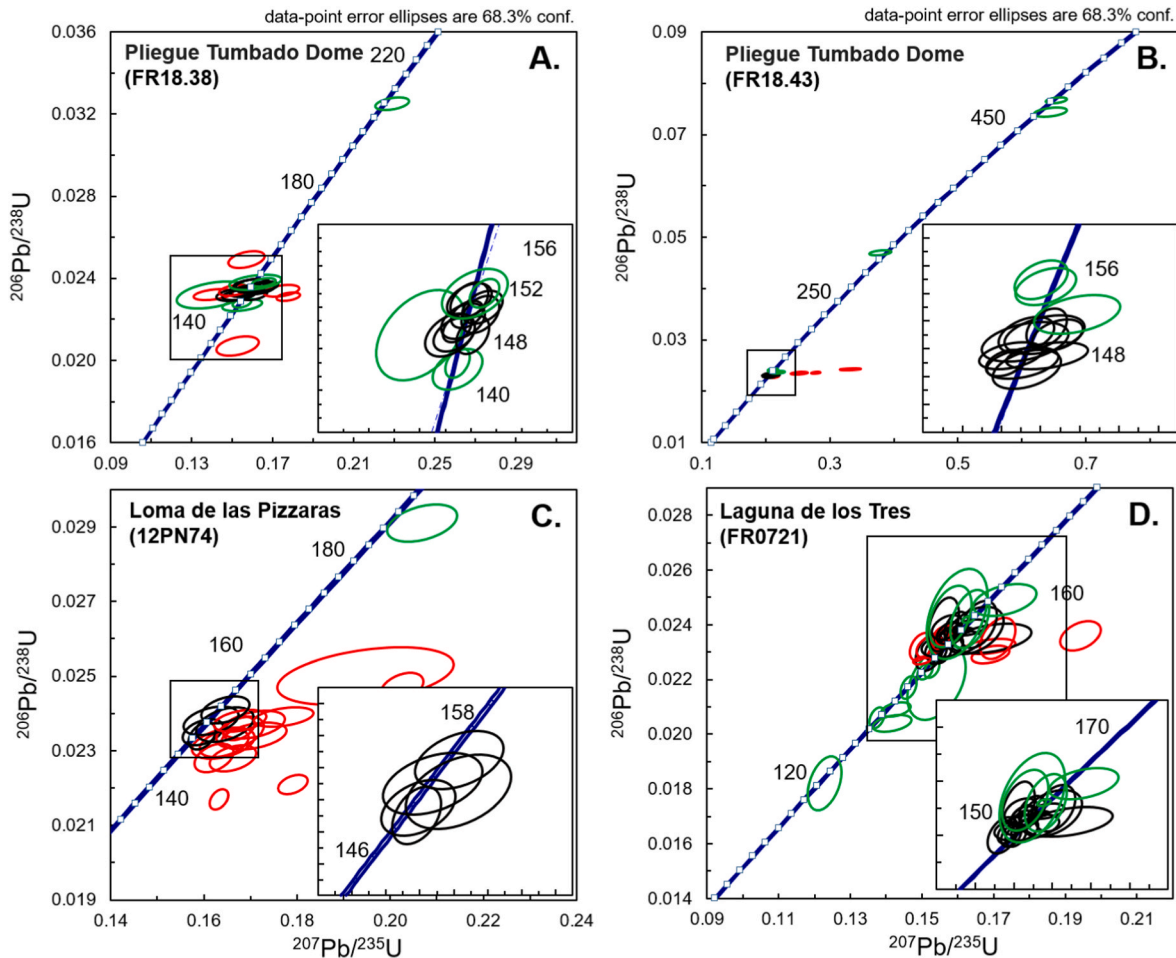


Fig. 5. Normal Concordia ($^{206}\text{Pb}/^{238}\text{U}$ vs $^{207}\text{Pb}/^{235}\text{U}$) diagrams for two samples from the Pliegue Tumbado Dome (A–B) and two rhyolites from the western samples (C–D). Three samples show clear inheritance. (A–C) Discordant analyses are shown as red rings. Concordant analyses are both green and black; only the black analyses are included in the calculated average age. Inset graphs are indicated by a black box within the larger Concordia diagram.

2001). However, we note that we obtain systematically younger U–Pb ages than those previously reported by Pankhurst et al. (2000) for this final (V3) episode.

The largest comparable dataset of in-situ ages for the EQC outside of El Chaltén was generated by SHRIMP analysis (e.g., Pankhurst et al., 2000). While we note that our samples are from a different EQC locality – the closest locality is El Unión dated at ~155 My, ~100 km south of El Chaltén – our youngest ages calculated have a maximum difference of ~6 My compared to the youngest ages reported by Pankhurst et al. (2000). However, more recent geochronology of rhyolitic domes of similar young age (146.5 ± 0.2 and 146.3 ± 0.2 Ma; Poblete et al., 2013) in the Chile Chico region using high precision dating by ID-TIMS gives us confidence in the importance and robustness of the younger zircon U–Pb ages for the El Quemado Complex (see also Malkowski et al., 2016).

Pervasive high-temperature alteration related to late-stage hydrothermal activity, in combination with the thermal effects relating to the emplacement of the Fitz Roy intrusive complex, made dating the volcanic rocks of the EQC in the Chaltén region challenging.

Disturbances in the U–Pb system of the zircon crystals are evident by the large proportion of discordant analysis within all samples analyzed in this study. However, Rb–Sr and $^{40}\text{Ar}/^{39}\text{Ar}$ age estimates consistently yield ages that are younger than those estimated with zircon U–Pb in the EQC and CASP (e.g., Féraud et al., 1999; Pankhurst et al., 2000). The age discrepancies between zircon U–Pb and the alkali feldspar and/or biotite Rb–Sr and $^{40}\text{Ar}/^{39}\text{Ar}$ studies reflect differences in the closure temperatures of the isotope system whereby the younger age estimates given by Rb–Sr and $^{40}\text{Ar}/^{39}\text{Ar}$ commonly record low-temperature, gradual

closure due to post-crystallization hydrothermal equilibration (Riley and Leat, 1999; Pankhurst et al., 2000). For the EQC, careful data assessment is important, but zircon U–Pb geochronology remains as the most reliable recorder of magmatic crystallization ages for volcanic rocks in this region which have undergone variable processes of alteration.

6.2. Inheritance documented by xenocrystic zircon cores

The preservation of xenocrystic cores within the EQC rhyolites in El Chaltén provides important constraints on both the source of the silicic magmas and on the timing of xenocrystic incorporation into the hosting magma. The values of zircon oxygen isotopes in the El Chaltén area are high for silicic rocks ($>8\text{‰ } \delta^{18}\text{O}$), indicating a significant crustal role in the generation of many of these rhyolites dated during this study (Seitz et al., 2018). Such high oxygen values are derived during partial melting of the source protolith and less likely derived during upper-crustal assimilation, as thermal considerations do not allow significant assimilation of surrounding wall rock into a cooling magma body within the upper crust (e.g., Glazner, 2007). Therefore, considering the elevated oxygen isotope values of the EQC magmas combined with the thermal limitations of assimilation, we favor the interpretation that xenocrystic zircons are inherited from a mid- to lower-crustal source during crustal anatexis.

The younger xenocrystic (potentially antecrystic; c.f. Miller et al., 2007) Jurassic zircon ages (~165–185 Ma) in the EQC rhyolites of El Chaltén overlap with the older magmatic episodes of the CASP in both

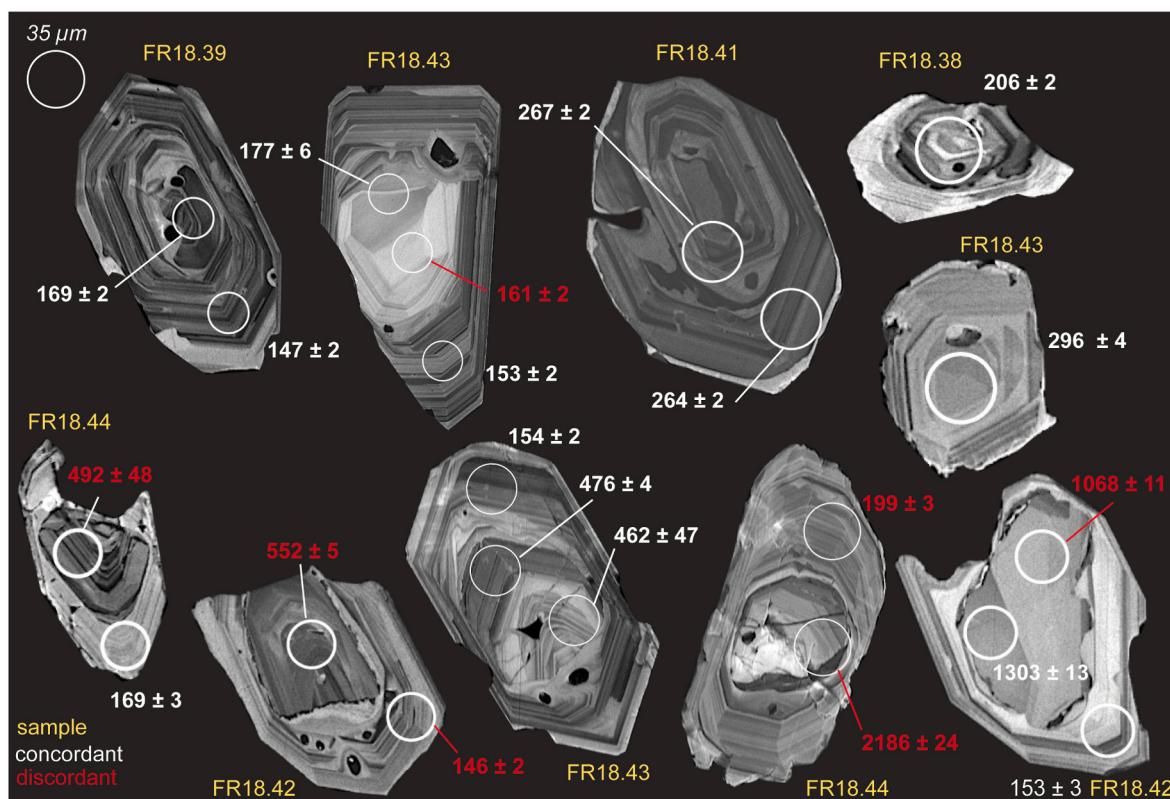


Fig. 6. Cathodoluminescent images of xenocrystic (inherited) zircon grains in the Pliegue Tumbado Dome. The size of crystals is indicated by the size of the LA-ICP-MS spot size (35 μ m). Xenocrystic grains which have discordant age analysis are also included to show the internal textures which often clearly indicate distinctly different internal zonation, when compared to the younger overgrowths.

Patagonia and the Antarctic Peninsula (Pankhurst et al., 2000; Riley et al., 2001, 2016). Similar igneous ages have not been documented in the Chaltén area. The distance between the EQC around El Chaltén and the oldest V1 (~181–188 Ma) units of the Marifil Formation of the North Patagonian Massif (ca. 700 km) or the Brennecke and Mount Poster Formations (ca. 1000 km during the Early Jurassic, cf. Riley et al., 2016) of the Antarctic Peninsula, and the V2 (~160–170 Ma) Chon Aike Formation of the Deseado Massif (ca. 300 km) is large. Thus, it is unlikely that the origin of the ~165–185 Ma ages in the Chaltén volcanic rocks is directly linked to a spatial overlap with those magmatic centers.

At the latitude of El Chaltén (49°S), xenocrystic zircons with ages of approximately 165–185 Ma are found in similar aged (~150 Ma) Jurassic rocks of the southern Patagonia Batholith (gneiss, gabbro, and granodiorite). Hervé et al. (2007a) initially proposed a temporal, spatial and genetic link between the granitoids (tonalite through granodiorite compositions) of the Southern Patagonian Batholith and the rhyolites of the EQC, based on overlapping ages and geochemical similarities (REE, trace elements, $^{87}\text{Sr}/^{86}\text{Sr}$ and ϵNd_t). However, intrusion ages of 185 Ma have not been found in the Southern Patagonian Batholith. Nevertheless, the outcrops are difficult to access, and sampling of this vast area is still largely incomplete despite the recent commendable efforts of Hervé et al. (2007a).

In El Chaltén, it is possible that the ages ranging from ~165 to 185 Ma could represent the early onset of magmatism related to active subduction. However, since there is no strong clustering of a single age in this range of xenocrystic cores in our dataset (~160–185 Ma), it is also possible that these ages could represent the geochemical mixing of two distinctly different zircon domains during the LA-ICP-MS analysis, related to the spatial resolution and the cumulative volume of ablated material. Therefore, without additional data, we cannot discern the origin of these Early-Middle Jurassic ages.

Determining the probable source(s) of the older xenocrystic zircons

(ca. 200 to 1.3 Ma) is challenging due to the lack of exposures of rocks with such age in the El Chaltén region. In many locations, the EQC unconformably overlies the Paleozoic EAMC basement, providing a discontinuity where roughly ~250 Ma of geologic history is missing (Giacosa et al., 2012a; Suárez et al., 2019a). Either the sources of xenocrystic zircon cores are extremely limited at the surface and have not been described as of yet, or they are not exposed at the surface and are hidden due to extensional faulting and subsequent deposition. To identify potential sources of inherited zircon, we first explore the location and ages of available igneous and metasedimentary basement exposures throughout southern Patagonia in the following section.

6.3. Review of the existing basement exposures in southern Patagonia

The igneous basement exposures are confined to the Deseado Massif and Tierra del Fuego along the eastern edge of southern Patagonia. The basement rocks in the west are predominantly metasedimentary (Fig. 7). The oldest igneous basement rocks of southern Patagonia range from the latest Proterozoic to the earliest Paleozoic and are the result of the initial stages of the Terra Australis Orogeny (Cawood, 2005; Hervé et al., 2010a), forming a fundamental silicic crustal component in southern Patagonia. The oldest dated samples are from boreholes in the Magallanes basement of Tierra del Fuego and the bordering regions of Chile (Fig. 7). Cambrian granitoids that have been variably metamorphosed into orthogneisses range from ~520 to 540 Ma (Söllner et al., 2000; Hervé et al., 2010a). Similarly, the Dos Hermanos amphibolite from the Rio Deseado Complex of the eastern Deseado Massif is ~540 Ma (Pezuchichi, 1978). The overlap of similar ages and compositions of the Dos Hermanos amphibolite with one of the Magallanes orthogneisses supports the interpretation of the occurrence of widespread Cambrian mafic calc-alkaline magmatism in southern Patagonia. Taken together with rocks in central and northwestern Argentina, the overlap in age and

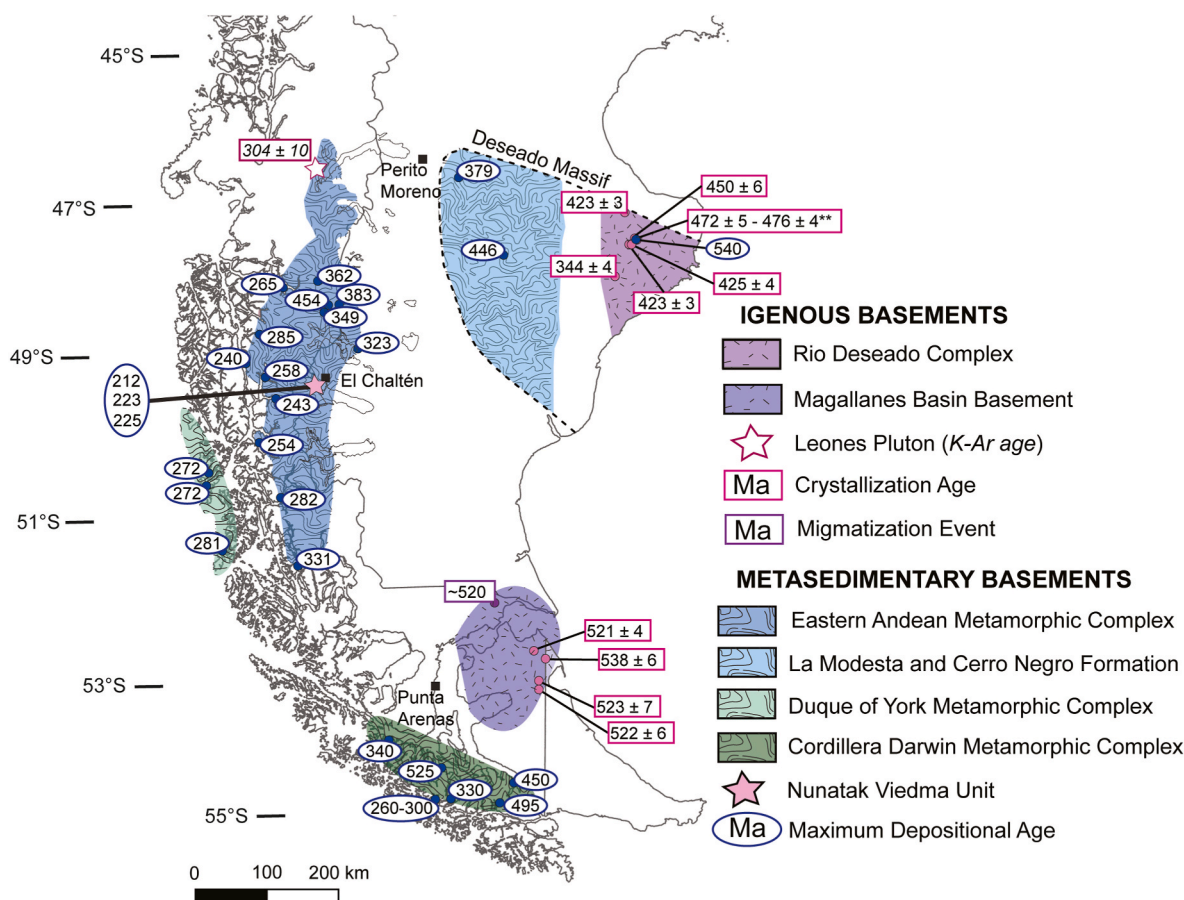


Fig. 7. Present day southern Patagonia basement rock locations with corresponding ages as determined by zircon U–Pb studies. Publications by regions include: Río Deseado Complex (Pankhurst et al., 2003); Magallanes Basin (Pankhurst et al., 2003; Hervé et al., 2010a); La Modesta Formation (Moreira et al., 2013), Cerro Negro Schist (Permuy-Vidal et al., 2014), the Eastern Andean Metamorphic Complex (Pezzuchi, 1978; Hervé et al., 2003; Augustsson et al., 2006), the Duque of York Metamorphic Complex (Hervé et al., 2003; Calderón et al., 2016), the Nunatak Viedma Unit (Suárez et al., 2019b), and the Cordillera Darwin (Hervé et al., 2010b). **crystallization ages were determined from granitoid cobbles separated from a Permian-aged conglomerate and therefore do not represent in-situ ages.

compositions suggests an extended spatiotemporal link of the Early Paleozoic Pampean orogenic cycle (~515–550 Ma) into southern Patagonia (Söllner et al., 2000; Pankhurst et al., 2003, 2014).

The Río Deseado Complex comprise the remaining older formations exposed in southern Patagonia. Although not sampled *in situ*, two granitoid cobbles sampled from a Permian conglomerate (La Golondrina Formation) were dated at 476 ± 4 and 472 ± 5 Ma (Fig. 7). The large size of the cobbles suggests that the source is nearby, though likely now covered. The mid-Ordovician ages support the emplacement of granitic magma within the eastern Deseado Massif (Pankhurst et al., 2003) that was contemporaneous with the Famatinian magmatism of the Sierra Pampeanas in central Argentina (Guido et al., 2004; González et al., 2011, 2018; Ramos and Naipauer, 2014; Rapela et al., 2018). The consistency of overlapping ages combined with geochemical and isotopic concentrations in granitoids from the North Patagonian Massif and the Sierra Pampeanas further support the continuity of the Famatinian belts into Patagonia, forming part of the Early Paleozoic margin of Gondwana (Pankhurst et al., 2003, 2014).

The younger granites of the Río Deseado Complex are of mid-Silurian to Carboniferous age (425–344 Ma; Pankhurst et al., 2003) (Fig. 7). The continuity of granitoids with similar ages in the eastern Deseado Massif with a dominate north-west trend extending into the North Patagonian Massif is taken to represent the presence of a widespread, subduction-related magmatic-arc, which crosses obliquely across southern Patagonia (Ramos, 2008; Moreira et al., 2013; Permuy-Vidal et al., 2014).

The youngest plutonic exposure in southern Patagonia is the Leones

Pluton, dated at 307 ± 10 Ma by K–Ar in muscovite (Fig. 7; De La Cruz and Suárez, 2006; Rojo et al., 2021b). Positioned in the northern-most sector of the EAMC (~46 °S), this plutonic suite is hypothesized to represent the migration of arc magmatism from its early-Carboniferous position in the Deseado Massif to a late-Carboniferous position within the present-day Andean region. This migration in arc magmatism ultimately results from the closure of the back-arc basin between the Antarctic Peninsula and the Patagonian region, in response to the westward drift of the Antarctic Peninsula relative to the late Paleozoic Gondwana margin (Rojo et al., 2021a, 2021b).

Basement exposures younger than the Río Deseado Complex have a sedimentary origin and were later regionally metamorphosed. The oldest metasedimentary units were probably deposited in a mid-Silurian volcanic arc, the existence of which is indicated by diachronic mid-Paleozoic forearc/foreland basin with clay and sandstone-clay marine sediments in the La Modesta Formation and Cerro Negro Formation in the east and turbidite sequences of the EAMC in the west (Moreira et al., 2005; Permuy-Vidal et al., 2014; Suárez et al., 2019a) (Fig. 7). Maximum sedimentation ages in the EAMC become younger as the deposition progressed westward into the Chilean exposures; the youngest maximum depositional age is 240 Ma (Hervé et al., 2003). At the farthest extent of the western Andean border, maximum depositional ages for the turbiditic succession of the Duque of York Metamorphic Complex partially overlap with the easternmost samples of the EAMC (~ca. 270 Ma; Hervé et al., 2003; Sepulveda et al., 2010) (Fig. 7). In the southernmost Fuegian Andes (~55°S), the Cordillera of Darwin Metamorphic Complex has detrital zircon patterns that are comparable to

those of the eastern domain of the EAMC (ca. 260–500 Ma, [Hervé et al., 2010b](#); [Calderón et al., 2016](#)).

Recently described outside of the Chaltén area are the youngest metamorphic rocks of the Nunatak Viedma unit, with a maximum depositional age of ~220 Ma ([Suárez et al., 2019b](#)). The dominance of detrital zircon age peaks (e.g., comprising ~50% of the age spectra) from Permian to Late Triassic require a proximal igneous source from an evolving magmatic arc. Based on paleogeographic reconstructions, primary sources are sourced from either southern Patagonia, the Antarctic Peninsula, or the Malvinas Islands ([Suárez et al., 2019b](#)).

[Rojo et al. \(2021b\)](#) depicts the depositional environment of the EAMC positioned in a back-arc basin setting with the turbidite sequences partially overlying oceanic crust (see Fig. 13 in [Rojo et al. \(2021b\)](#)), suggesting the extent of the oldest crystalline basement in the Deseado Massif is extremely restricted. This configuration would imply that the lower crust starting from the Carboniferous plutonic units in the Deseado Massif extending until the present-day Andean coastal position is largely comprised of metamorphosed basaltic sequences underlying the turbidites of the EAMC ([Fig. 7](#)). This interpretation provides as a possible configuration for the Andean lower crust; in the following sections, we explore the possibility of other configurations based on the available zircon xenocryst data.

6.4. Inherited xenocrystic zircon cores of southern Patagonian igneous units

Zircon's ability to record the timing of crustal events depends on zircon saturation that results in the precipitation of new magmatic zircon, the re-equilibration of pre-existing magmatic zircon during a

metamorphic event, or the precipitation of new metamorphic zircon. Using inherited zircon age populations in a given region provides insight into unexposed portions of the lower crust when it is incorporated into younger magmas that do become exposed (e.g., [Miller et al., 1992](#); [Bryan et al., 2008](#); [Farina et al., 2018](#)). Our analyzed xenocrystic ages preserved in the EQC rhyolites, when compared with a compilation of published xenocrystic ages documented from volcanic and plutonic rocks (Cenozoic to Paleozoic crystallization ages) throughout southern Patagonia, show that magmatism was continuous from the early Paleozoic until present day. All studies included in this summary use an in-situ method (LA-ICP-MS or SHRIMP) for zircon U–Pb ages, and therefore are comparable datasets.

There is considerable overlap in inherited zircon age spectra between the Pliegue Tumbado Dome (El Chaltén) with those of other igneous rocks found throughout southern Patagonia. Various sources include ([Fig. 8](#)): (1) the Miocene Cerro Pampa adakite ([Kay et al., 1993](#); [Orihashi et al., 2013](#)); (2) calc-alkaline plutonic bodies of the Miocene Torres del Paine; ([Müntener et al., 2018](#)); (3) other Jurassic volcanic rocks exposed within the CASP ([Pankhurst et al., 2000](#); [Moreira et al., 2009](#); [Malkowski et al., 2016](#); [Muller et al., 2021](#)); (4) numerous Jurassic granitoids of the Patagonia batholith ([Hervé et al., 2007a](#)); (5) the Permian granites and granodiorites in Tierra del Fuego ([Castillo et al., 2017](#)); (6) the Paleozoic granitoids of the Río Deseado Complex ([Pankhurst et al., 2003](#)); and (7) two crystalline basement samples in the Magallanes Basin of Tierra del Fuego ([Hervé et al., 2010a](#)). Units that contain xenocrystic zircons range age from the 12 My Cerro Pampa adakite to the ~470 My granitoids of the Río Deseado Complex and cover a broad range of compositional variability. There is no obvious correlation between age or composition and the prevalence of preserved xenocrystic zircons.

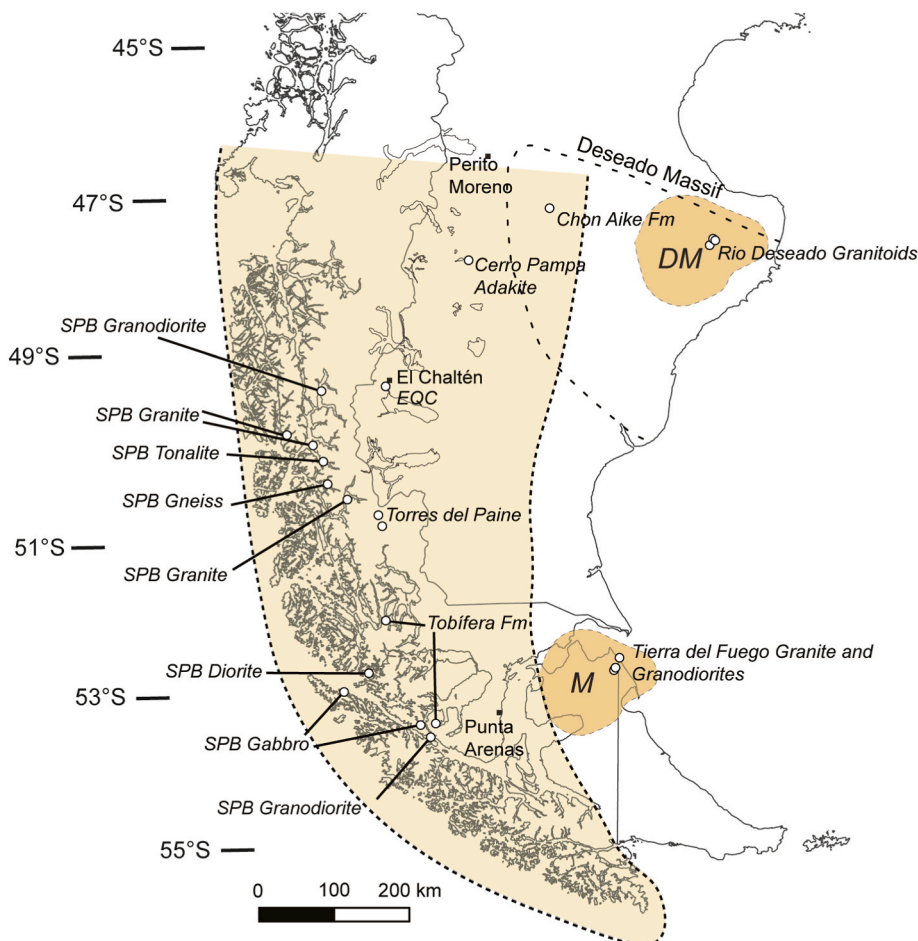


Fig. 8. Schematic of southern Patagonia showing the corresponding localities of igneous rocks which host xenocrystic (inherited) zircon ages. The three yellow areas separate the main regions based on current basement rock exposures and their relation to the Paleo-Pacific Gondwanan margin: the Paleozoic igneous basements of the Deseado Massif (DM) and the Magallanes Basement (M) of Tierra del Fuego, and the (meta)sedimentary cover of the Paleo-Pacific Gondwanan margin (greater Andean region) which is intruded by the younger Mesozoic to Cenozoic igneous units. Source publications per igneous unit are detailed in the text.

We compare the various sources of documented zircon inheritance and age spectra frequency of three separate regions: the paleo-Gondwanan continental active-margin (present day Andes), the Deseado Massif, and the Magallanes Crystalline basement (Fig. 8). These areas are distinguished based on potential changes in contributing basement source relating either to crystalline basement regions or the active Paleomargin of Gondwana. Separation between the Río Deseado Complex and the Tierra del Fuego region is made to show potential overlap in xenocrystic ages between regions of known igneous basement sources and the paleo-Gondwanan continental active-margin region, in which the only known basement is metasedimentary.

Available inherited zircon age data preserved in the compositionally and temporally different igneous units throughout the southern Patagonia area is scarce because of the vast aerial extent of southern Patagonia. Where xenocrystic ages have been reported, they are often not fully discussed with respect to potential rock sources (e.g., Pankhurst et al., 2000; Moreira et al., 2009; Hervé et al., 2007a; Malkowski et al., 2016). Our new compilation of inherited ages reveals a clustering of age groups (Fig. 9a).

The first group lies along the paleo-Gondwanan continental active-margin. Here, the oldest known exposed basement is metasedimentary and has an average depositional age of >250 Ma and older depositional ages of >350 Ma recorded along the eastern Andean margin (Fig. 7). This group also includes all the Cenozoic igneous units and almost all Mesozoic (excluding the Permian Tierra del Fuego granitoids) which preserve the youngest inherited zircon ages (<400 Ma) in addition to sparse older inherited zircon ages (400–1650 Ma) (Fig. 9b). The first cluster of inherited ages in many of the igneous units are between 200 and 300 Ma (Fig. 9b). About 50 km east of the modern Andean margin, the Cerro Pampa adakite preserves a copious number of inherited ages in this range of Late-Triassic to Permian. The second cluster of ages found

in many of the units is the 450–500 Ma. The third cluster, which is less pronounced than the other clusters, is the 550–600 Ma age group and is expressed in units that are found over a large areal extent in southern Patagonia. Ages older than 600 Ma are rare and widely distributed, but the oldest inherited ages measured in two units (the Chon Aike Formation and the Southern Patagonian Batholith, Pankhurst et al. (2000) and Hervé et al., 2007a, respectively), range from 1601 ± 20 to 1673 ± 7 Ma (Fig. 9b).

The second group includes three granitoids of the Río Deseado complex in the eastern Deseado Massif (Pankhurst et al., 2003). In the Dos Hermanos muscovite leucogranite (450 ± 5 Ma), two analyses gave ages of 653 ± 7 Ma and 835 ± 13 Ma (Fig. 9c). Inherited age analyses for two samples in the El Sacrificio granite (425 ± 4 Ma, two mica-garnet leucogranite) give 662 ± 7 Ma, 831 ± 9 Ma, 884 ± 16 Ma, 1056 ± 19 Ma, and 1317 ± 24 Ma. Two inherited ages of 935 ± 50 and 1014 ± 14 Ma were analyzed in the granite cobbles (crystallization ages of ~454–472 Ma) sampled from La Golondrina Formation. No single age group dominates the in the Río Deseado Granites, but the older inheritance ages (≤ 1.3 Ga) indicate older crust beneath the eastern Deseado Massif (Fig. 9c). S-type affinities indicated by the peraluminous nature (two-micas) of the granitoids within the Río Deseado complex support a crustal origin (Pankhurst et al., 2006).

The third group includes the Permian granitoids (~250–260 Ma; Castillo et al., 2017) and two Cambrian-aged crystalline basement samples in Tierra del Fuego (~515–540 Ma; Hervé et al., 2010a) (Fig. 7). The Permian units are closely spatially correlated to the Magallanes basement orthogneisses and include multiple inherited zircons of a similar age, indicating melting of the Magallanes basement. The three Permian granitoids in Tierra del Fuego record zircon inheritance of 510–660 Ma and 960 Ma (Fig. 9d) (Castillo et al., 2017). The dominance of inherited ages ~520–550 Ma is likely linked to melting and/or

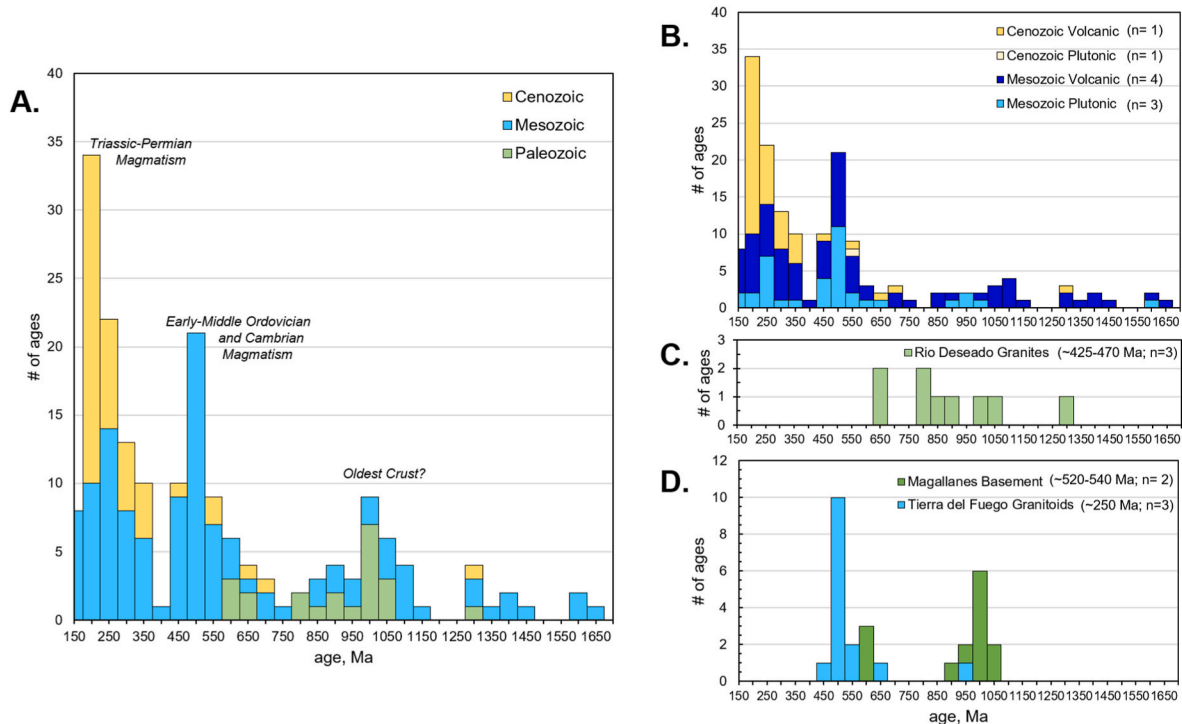


Fig. 9. (A) Histogram of Inheritance Ages throughout southern Patagonia colored by Era of the host rock (Cenozoic, Mesozoic, and Paleozoic). The histograms are separated into the three regions as defined in text: (B) The Paleo-Pacific Gondwanan margin with ages separated by Era and further by volcanic or plutonic origin, (C) the Río Deseado basement granitoids of Silurian to Ordovician age, within the eastern Deseado Massif, and (D) the granitoids within Tierra Del Fuego, including both the Cambrian Magallanes Basement and younger Triassic units. The oldest (Paleozoic) granitoids, which predominately host the oldest ages of xenocrystic (inherited) zircons, intruded within the crystalline basement regions. References to published xenocrystic zircon data includes Pankhurst et al. (2000), Pankhurst et al. (2003), Hervé et al. (2007a), Moreira et al. (2009), Hervé et al. (2010a), Orihashi et al. (2013), Castillo et al. (2017), Malkowski et al. (2016), Müntener et al., (2018), and Muller et al. (2021).

significant assimilation of the Magallanes basement orthogneiss, while the older age hints at a possible older underlying crust in the Tierra del Fuego region. Elevated zircon oxygen isotope values ($>8\text{‰ } \delta^{18}\text{O}$) for these three granites and the inherited zircon zones indicates a significant crustal input into the generation of these granites (Castillo et al., 2017). The Cambrian migmatitic granitoid sampled at Monte Aymond shows peaks at ca. 950–1100 Ma and 560–650 Ma, suggesting the migmatization and involvement of a Grenvillian and Brasiliano material in the protolith (Hervé et al., 2010a).

6.5. Assessing the nature of the lower crust of southern Patagonia

Due to the lack of exposures and overall knowledge on the origin of southern Patagonia, any robust assessment on the compositional spectrum and geologic history of the basement is much more complicated in comparison to studies conducted worldwide in places where cratons are the most probable sources of zircon inheritance (e.g., Cretaceous Granitoids of Western USA, Miller et al., 1992; Sierra Madre Occidental, Mexico, Bryan et al., 2008). Another challenge in determining the age and configuration of the lower crust in the Andean region is the lack of overlap between studies of the Deseado Massif and the igneous rocks of the Andes which primarily focus on the Patagonian Batholith. Studies concentrated on the Andes often illustrate the lower crust as a thick, Paleozoic undifferentiated crust with no easterly connection to either the Deseado Massif or the corresponding Northern Patagonian Massif (e.g., Rolando et al., 2002; Hervé et al., 2007b; Fosdick et al., 2013; Ghiglione et al., 2019). In contrast, studies that focus on provenance of the metasedimentary basement of the western Deseado Massif (La Modesta or Cerro Negro Formation; Moreira et al., 2013; Permuy-Vidal et al., 2014) or the Eastern Andean Metamorphic Complex (EAMC) (Hervé et al., 2003; Augustsson and Bahlburg, 2003; Augustsson et al., 2006; Augustsson and Bahlburg, 2008) often interpret and describe the primary depositional environment of the sediments without further considerations about composition or age descriptions of the crust that they were deposited on.

Active magmatism from the Early Paleozoic until present day in southern Patagonia is supported by both the known exposures of igneous basement outcrops and widespread inheritance of older xenocrystic zircons (Fig. 10). Although the compilation of xenocrystic data covers time periods from Jurassic through Mesoproterozoic, we focus on the three most prominent histogram peaks in the data for discussion: (1) abundant Triassic-Permian (200–300 Ma) inherited zircons along the Paleo-Pacific Gondwanan margin; (2) the existence of widespread Early-Middle Ordovician to Cambrian inherited ages throughout southern Patagonia (~460–540 Ma); (3) there is an older (~1.0 Ga) crust below the Deseado Massif and the Tierra de Fuego region which may extend beneath present-day Andes.

Current paleogeographic reconstructions orient the Antarctic Peninsula along the southwest end of South American, forming the southwest margin of Gondwana from late Paleozoic until early Mesozoic (e.g., Pankhurst et al., 2003; Hervé et al., 2003; Hervé et al., 2006; Calderón et al., 2016; Riley et al., 2016; Suárez et al., 2019a; Suárez et al., 2019b; Navarrete et al., 2019; Riley et al., 2020; Bastias et al., 2021). Considering this tectonic configuration and the correlation of overlapping magmatic and tectono-metamorphic events between the two regions, we include the Antarctic Peninsula as potential sources of xenocrystic zircon from Permian until the Jurassic (Fig. 10a–c).

(1) Abundant Triassic-Permian (200–300 Ma) inherited zircons along the Paleo-Pacific Gondwanan margin (Figs. 9b and 10b–c). The presence of a well-developed magmatic arc related to continuous subduction is supported by numerous Permian through Triassic calc-alkaline intrusive bodies in Patagonia and in the Antarctic Peninsula (Fig. 10b–c). The lack of subduction related magmatism in the southern Andean region of Chile and Argentina is proposed to result from the formation of an

autochthonous terrain between South America and the Antarctic Peninsula (e.g., Burton-Johnson and Riley, 2015; Navarrete et al., 2019). The abundance of Triassic to Permian inherited ages analyzed in Cenozoic igneous rocks in southern Patagonia reflect this period of continuous magmatism along the Paleo-Pacific Gondwanan margin (Fig. 10b–c).

During the Late-Triassic (200–220 Ma), authors have proposed the existence of a segmented flat-slab to explain a possible inward migration of subduction related magmatism exposed as granitoids in the eastern Deseado Massif (~208 Ma La Leona granite; Navarrete et al., 2019) and in the North Patagonian Massif (~202–220 Ma Central Patagonian Batholith; Rapela and Pankhurst, 1992; 1996; Zaffarana et al., 2014) (e.g., Navarrete et al., 2019; Bastias et al., 2021) (Fig. 10b). At the same time, numerous igneous units oriented along the Andean margin preserve copious xenocrystic zircons of 202–222 Ma ages (e.g., Cerro Pampa adakite, EQC, and the Southern Patagonian Batholith). The Nunatak Viedma unit provides a potential detrital source of Late-Triassic to Permian (ca. 208 to 300 Ma; Suárez et al., 2019b) ages for the abundant xenocrysts analyzed within the EQC rhyolites ($n = 13$; this study and Malkowski et al., 2016). However, due to the restricted extent of this formation and the expansive spatial distribution of igneous units with inherited zircons with these ages, it is unlikely that this formation provided these ages for all igneous units considered here. Either the Late-Triassic sedimentary basins in southern Patagonia are more extensive than previously thought (e.g., Fig. 4 in Riley et al., 2020), or these xenocrystic ages represent the position of arc magmatism associated with normal subduction, requiring an alternative explanation for the sparsely exposed Late-Triassic granitoids in the eastern margin of southern Patagonia (Fig. 10b).

The Early to Middle-Triassic (220–250 Ma) magmatic arc is established in the Antarctic Peninsula (Millar et al., 2002; Flowerdew et al., 2006; Riley et al., 2012, 2020; Bastias et al., 2020), but is not recorded in Patagonia (Fig. 10b). Similarly, xenocrystic zircons of this age are less abundant in southern Patagonia and are represented primarily in the Cerro Pampa adakite (Orihashi et al., 2013).

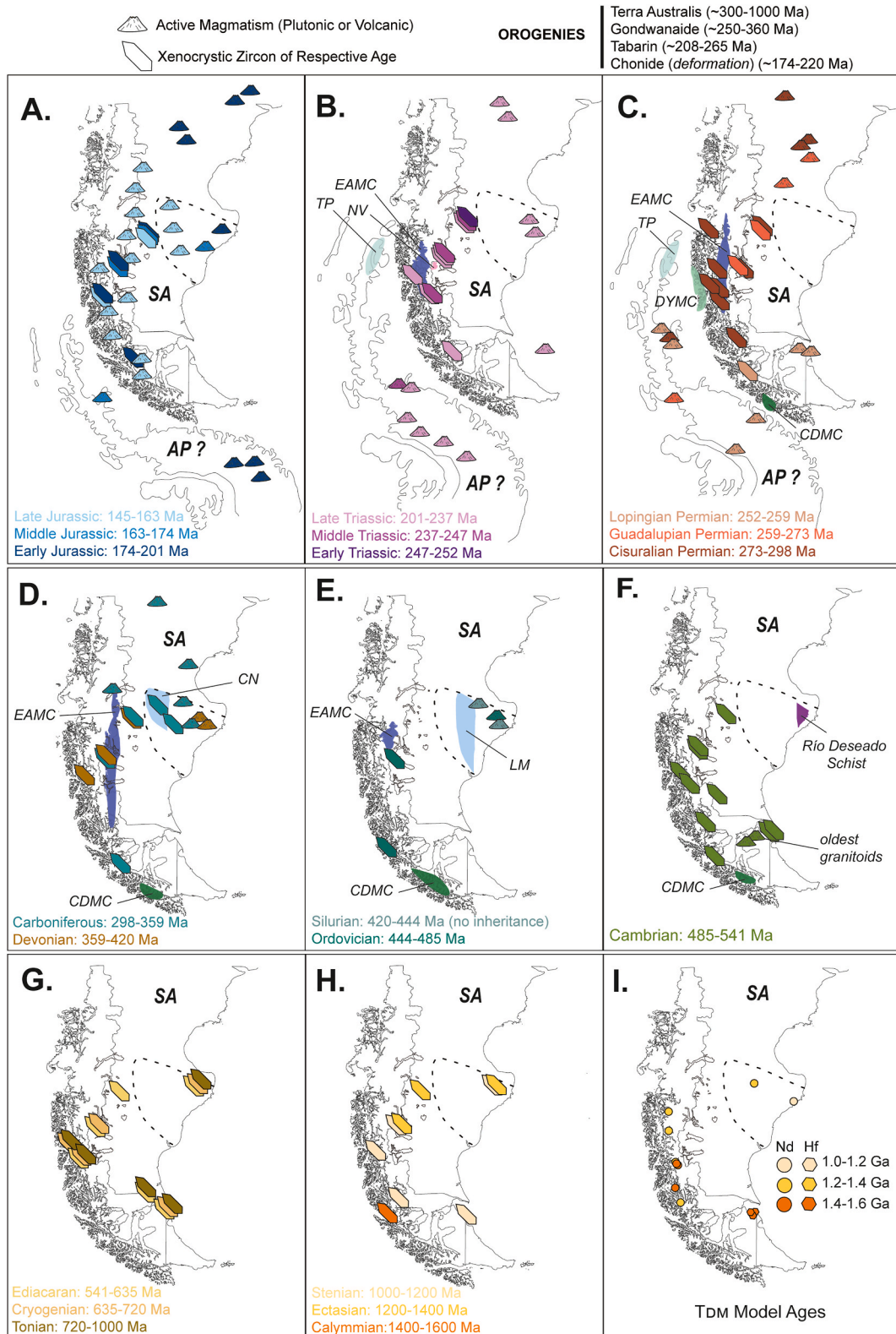
The presence of Permian arc-related magmatism is extensive throughout the western Gondwanan margin with numerous granitoids in the North Patagonian Massif (ca. 250–295 Ma; Varela et al., 2005; Pankhurst et al., 2006; Ramos, 2008; Castillo et al., 2017), Tierra del Fuego (ca. 255 Ma; Castillo et al., 2017), and in the Antarctic Peninsula (ca. 255–280; Millar et al., 2002; Riley et al., 2012) (Fig. 10c). Interestingly, the igneous units are predominately Lopingian in age (251–259 Ma), whereas the xenocrystic zircon in the Andean region of southern Patagonia are of Cisuralian age (273–298 Ma). The EAMC and the Duque de York metamorphic complex provide the most probably detrital source of early Permian ages (Augustsson et al., 2006; Hervé et al., 2010b; Sepulveda et al., 2010; Suárez et al., 2019a). Alternatively, the early Permian xenocrystic ages along the Andean margin could be sourced from a primary igneous source, representing a subduction-related magmatic arc within the Andean region which is first indicated by the late-Carboniferous Leones Pluton (ca. ~304 Ma; De La Cruz and Suárez, 2006; Rojo et al., 2021b). The first indication of the magmatic arc within the Antarctic Peninsula is represented by the oldest early Permian granitoids dated at ~270 Ma (ca. 272 Ma diorite gneiss, Riley et al., 2012).

(2) Early-Middle Ordovician to Cambrian xenocrystic ages are widespread throughout southern Patagonia (~460–540 Ma). Similar ages of inheritance suggest a common lower crustal source (or, more likely, a shared tectonic history), which relates particularly to igneous units in the Río Deseado Complex and the Permian Granitoids in the Tierra del Fuego region (Fig. 10e–f). These ages parallel the two major orogenic cycles recorded within South America along the western margin of Gondwana: the Famatinian (~400–480 Ma) and the Pampean orogeny

(~530–550 Ma) (Söllner et al., 2000.; Guido et al., 2004; Schwartz et al., 2008; Casquet et al., 2012; Weinberg et al., 2018; Rapela et al., 2018). It is possible that contemporaneous magmatism of these two major orogenic cycles is recorded within the lower crust of the Andean region of southern Patagonia and are now present as inherited zircons within the CASP (EQC and

Tobífera Formation), the South Patagonian Batholith, and the Cerro Pampa adakites.

(3) An older (~1.0 Ga) crust below the Deseado Massif and the Tierra de Fuego region that may extend beneath present-day Andes. Xenocrystic ages in the oldest igneous units of southern Patagonia, including the Río Deseado complex and the Magallanes



(caption on next page)

Fig. 10. Simplified depiction of southern Patagonia magmatism (intrusive and extrusive) through time with the reconstruction of the Antarctic Peninsula depicted from Jurassic through Permian times (geographic reconstructions based on Pankhurst et al. (2000) Hervé et al. (2003), Calderón et al. (2016), Navarrete et al. (2019), Suárez et al. (2019a); Bastias et al. (2021), and references therein). See reviews in Suárez et al. (2019a) for references to timing of orogenic events. (A) Widespread CASP volcanism during the Jurassic with sparse Early Jurassic xenocrystic ages throughout the Andean region. Onset of subduction related magmatism within the Southern Patagonian Batholith begins in the Late Jurassic. (B–C) The inheritance of Triassic to Permian xenocrystic zircons is primarily concentrated along the western margin of southern Patagonia and correlates to active magmatism which is recorded in exposed in the Northern Patagonian Massif, Antarctic Peninsula and Tierra del Fuego. Multiple sedimentary basins record detrital zircon of these ages, including the Eastern Andean Metamorphic Complex, the Duque of York Metamorphic Complex, the Trinity Peninsula Group, and the Nunatak Viedma, 10D-E. A Mid to Late Paleozoic arc is represented by the Río Deseado Granites. Inherited ages of corresponding ages are present in the Tierra del Fuego granites and along the Andean margin which suggests for widespread Cambrian and Early-Middle Ordovician magmatism. The westerly migration of the sediments in response to the Paleozoic arc is seen with the deposition of the La Modesta Formation in the east and the continuation in time towards the west with the later disposition of the sediments comprising the Eastern Andean Metamorphic Complex. (F) Widespread Cambrian magmatism exposed as the granites in Tierra del Fuego and the metamorphism in the Deseado Massif region (Río Deseado schist). (G) The oldest, most abundant xenocrystic zircon of Neoproterozoic age are analyzed in the oldest exposed, Paleozoic basements of southern Patagonia. (H–I) Older xenocrystic zircons of Mesoproterozoic age are found throughout southern Patagonia, but similarly old initial neodymium and hafnium depleted mantle model ages from zircon studies support for the presence of a 1.2–1.6 Ga crust (references in text). Abbreviations: SA (South America), AP (Antarctic Peninsula), EAMC (Eastern Andean Metamorphic Complex), TP (Trinity Peninsula Group), NV (Nunatak Viedma), DYMC (Duque of York Metamorphic Complex), CDMC (Cordillera Darwin Metamorphic Complex), CN (Cerro Negro Formation), LM (La Modesta Formation).

crystalline basement, indicate an old crustal component ranging from >800 Ma to 1300 Ma, with a prominent clustering of ages at 1.0 Ga. However, ages older than 800 Ma are sparsely distributed throughout southern Patagonia in the younger igneous units, with zircons dated in many of igneous units described above (the Pliegue Tumbado Dome, the Tobífera Formation, the Southern Patagonian Batholith, the Cerro Pampa adakite, the Río Deseado granitoids (El Sacrificio granite) (Fig. 10f–g). With no single age group dominating the dataset, it is difficult to correlate the ages with a single geologic event. However, the inheritance of >1.0 Ga zircons throughout southern Patagonia (Fig. 10h) agrees well with >1.0 Ga neodymium and hafnium depleted mantle model ages which have been calculated across southern Patagonia from both igneous (CASP, Pankhurst and Rapela, 1995; Río Deseado Complex, Pankhurst et al., 2003; Southern Patagonian Batholith, Hervé et al., 2007a; Permian Tierra del Fuego Granitoids; Castillo et al., 2017) and metasedimentary rocks (Río Deseado Complex, Pankhurst et al., 2003). The combination of zircons of Grenvillian age and depleted mantle neodymium and hafnium model ages sourced throughout the Andean region and extending into the Deseado Massif supports similar lower crustal rocks beneath southern Patagonia at these latitudes (e.g., Ramos, 2010).

Based on the broad spread in ages and the similarity between the igneous versus the metasedimentary rocks of the Andes which show a typical “Gondwanan signature” (e.g., Hervé et al., 2003; Suárez et al., 2019a), we also consider that ages ranging from >800 to 1600 Ma are sourced from melting of a widespread metasedimentary unit in the lower crust (Fig. 10g–h). It is possible that the older xenocrystic ages present in the igneous units along the Paleo-Pacific Gondwanan margin have been initially derived from melting of a lower metasedimentary source (e.g., EAMC or La Modesta) and that the detrital grains were derived by weathering and erosion of the oldest igneous units from the Deseado Massif and Tierra del Fuego. An argument against a (primary) metasedimentary source for xenocrystic zircon in the EQC from the El Chaltén region comes from the textures of the inherited cores: CL-imaging shows that the cores are not rounded and therefore do not seem to indicate significant surface transport (Fig. 6). Permy-Vidal et al. (2014) concluded that any Devonian igneous sources (Río Deseado Complex) of detrital zircons for the Cerro Negro Formation had to have been transported approximately 200–250 km from the hypothesized paleobasin, and zircons traveling this distance should be significantly rounded and fractured. Considering a potential EAMC source for the inherited zircon grains, we can follow the same line of arguments: if EAMC detrital grains are primarily sourced from the Río Deseado Complex or secondarily sourced from erosion of the La Modesta Formation, then either transport was overall limited – which means these ages must be readily available for depositional source and the primary

igneous source is close – or the grains are instead inherited from a deeper magmatic source with limited dissolution.

To test the overall origin of these sparse older inherited cores (>800 Ma), additional zircon isotopic studies using *in situ* techniques, predominantly oxygen and hafnium isotope studies, which provide isotopic tracers on the source and origin, need to be applied to both the zircons in the metasediments of the La Modesta formation and the EAMC. This would allow them to be compared to those inherited by younger magmatic rocks. In addition, future research which incorporates zircon xenocryst data from the Antarctic Peninsula, the North Patagonian Massif, and Malvinas Islands would provide additional spatio-temporal constraints on the evolution of the western Gondwanan margin.

Magmatic events evidenced by outcrops of granitoids in the Río Deseado Massif and by inherited zircons with Silurian, Devonian, and Carboniferous ages are consistent between southern Patagonia, northern Patagonia, and west Antarctica. The consistency in ages throughout this vast region supports that these areas were autochthonous to the margin of Gondwana throughout the Paleozoic into the Mesozoic (Pankhurst et al., 2003).

7. Conclusions

We present new U–Pb zircon ages (in-situ LA-ICP-MS) for 16 silicic volcanic rocks from the El Quemado Complex in the region of El Chaltén. The obtained ages range from 147 to 153 Ma. Our results correspond to the youngest episode of Jurassic volcanism in the Chon Aike Silicic LIP.

We identify a series of inherited zircon cores. CL textures show that the inherited zircon cores are both igneous and metamorphic and are characteristically overgrown by Jurassic magmatic rims. These xenocrystic cores yield a large age range from 163 Ma to >1 Ga.

The use of inherited zircon age populations in a given region can provide insight into unexposed portions of the crust. We compiled data on xenocrystic zircons from various magmatic suites throughout southern Patagonia, including the Patagonian Batholith and the Deseado Massif, among others, to help identify and characterize unexposed basement and/or lower crustal sections.

The presence of inherited cores and a certain systematic age distribution in these magmatic suites both throughout the Andean and the extra-Andean regions supports the presence of old unexposed basement (s). The oldest crust comprising the basement is likely >1.0 Ga, as suggested by the widespread existence of inherited cores together with published neodymium and hafnium depleted mantle model ages (Pankhurst and Rapela, 1995; Pankhurst et al., 2003; Hervé et al., 2007a; Castillo et al., 2017). Younger zircon inheritance ages are the result of past magmatic (and metamorphic) events of the Terra Australis Orogen.

The silicic volcanic rocks of the EQC studied here in El Chaltén presents a special case for the study of inheritance because they appear to reflect magmas generated in a crustal anatexis regime (Seitz et al.,

2018). Understanding the nature of xenocrystic zircon by combining both their age and geochemistry has the potential to help unravel the complex history of basement blocks in southern Patagonia. To deduce the role of zircon inheritance and overall incorporation of xenocrystic grains into silicic magmas – including both the extrusive eruptions or their intrusive counterparts – more systematic *in situ* studies that document both core and rim analyses of large populations of zircons per given sample are necessary. A combination of oxygen and hafnium isotope and trace element analyses would further help to recognize specific rock source contributions.

Authorship statement

Author Contributions: M. Foley for data compilation, data analysis, writing and reviews, and figures. Z. Guillermin for her fieldwork and part of the zircon data acquisition. B. Putlitz and L. Baumgartner for field work, writing and reviews.

Declaration of competing interest

The authors declare that they have no known competing financial interests or personal relationships that could have appeared to influence the work reported in this paper.

Acknowledgements

We acknowledge S. Leresche, P. Nescher, and S. Seitz for their contribution for field work, sample collection, sample processing, and data collection during the years 2007–2018. This research is indebted to Andres Kosmal (El Chaltén, Argentina) for his friendly support in El Chaltén and in the field. We thank the authorities of the Parque Nacional de los Glaciares (Argentina) for permission to sample and their hospitality. The U–Pb measurements were made possible with the assistance of A. Ulyanov (UNIL). We thank S.P. Gaynor suggestions to earlier versions of this manuscript and to M.D. Acosta for additional edits and grammatical revisions. Final versions of this manuscript benefited from thoughtful discussions and contributions from E.M. Renda. This research is funded by the Swiss National Science Foundation (200021_175808 to BP). We lastly thank R.J. Suárez and two anonymous reviewers for their detailed suggestions and comments which greatly improved the original manuscript. We also acknowledge the editorial support from A. Folguera.

Appendix A. Supplementary data

Supplementary data to this article can be found online at <https://doi.org/10.1016/j.jsames.2021.103690>.

References

- Augustsson, C., Bahlburg, H., 2003. Active or passive continental margin? Geochemical and Nd isotope constraints of metasediments in the backstop of a pre-Andean accretionary wedge in southernmost Chile (46°30' – 48°30'S). In: Cann, M.C., T, Saintot, A. (Eds.), *Tracing Tectonic Deformation Using the Sedimentary Record*, vol. 208. Geological Society of London, Special Publications, pp. 253–268.
- Augustsson, C., Bahlburg, H., 2008. Provenance of late Palaeozoic metasediments of the Patagonian proto-Pacific margin (southernmost Chile and Argentina). *Int. J. Earth Sci.* 97, 71–88.
- Augustsson, C., Münker, C., Bahlburg, H., Fanning, M., 2006. Provenance of late Palaeozoic metasediments of the SW South American Gondwana margin: a combined U–Pb and Hf-isotope study of single detrital zircons. *J. Geol. Soc.* 163, 983–995.
- Baker, P.E., Rea, W.J., Skarmeta, J., Caminos, R., Rex, D.C., 1981. Igneous history of the andean Cordillera and Patagonian plateau around latitude 46° S. *Phil. Trans. Roy. Soc. Lond.* 303, 105–149.
- Bastias, J., Spikings, R., Ulyanov, A., Riley, T., Burton-Johnson, A., Chiaradia, M., Baumgartner, L., Hervé, F., Bouvier, A.-S., 2020. The Gondwanan margin in west Antarctica: insights from late Triassic magmatism of the Antarctic Peninsula. *Gondwana Res.* 81, 1–20.
- Bastias, J., Spikings, R., Riley, T., Ulyanov, A., Grunow, A., Chiaradia, M., Hervé, F., 2021. A revised interpretations of the Chon Aike magmatic province: active margin origin and implications for the opening of the Weddell Sea. *Lithos* 386–387.

- Bindeman, I.N., Melnik, O.E., 2016. Zircon survival, rebirth and recycling during crustal melting, magma crystallization, and mixing based on numerical modeling. *J. Petrol.* 57, 437–460.
- Bryan, S.E., Ferrari, L., Reiners, P.W., Allen, C.M., Petrone, C.M., Ramo-Rosique, A., Campbell, I.H., 2008. New insights into crustal contributions to large-volume rhyolite generation in the mid-Tertiary Sierra Madre Occidental province, Mexico, revealed by U–Pb geochronology. *J. Petrol.* 49, 47–77.
- Burton-Johnson, A., Riley, T.R., 2015. Autochthonous v. accreted terrane development of continental margins: a revised *in situ* tectonic history of the Antarctic Peninsula. *J. Geol. Soc.* 172, 822–835.
- Calderón, M., 2006. *Petrogenesis and Tectonic Evolution of Late Jurassic Bimodal Magmatic Suites (Sarmiento Complex) and Migmatites (Puerto Edén Igneous Metamorphic Complex) in the Southern Patagonian Andes, Chile*. PhD Thesis. Departamento de Geología, Universidad de Chile, p. 170.
- Calderón, M., Hervé, F., Fanning, C.M., 2004. Late Jurassic birth of the Rocas Verdes basin at the sarmiento ophiolitic complex: evidence from zircon U–Pb SHRIMP geochronology. In: Carcione, F., Donda, F., Lodolo, E. (Eds.), *GEOSUR International Symposium on the Geology and Geophysics of the Southernmost Andes, the Scotia Arc and the Antarctic Peninsula*, vol. 45. Bolletino di Geofisica Teorica ed Applicata, pp. 15–18.
- Calderón, M., Fildani, A., Hervé, F., Fanning, C.M., Weislogel, A., Cordani, U., 2007. Late Jurassic bimodal magmatism in the northern sea-floor remnant of the Rocas Verdes basin, southern Patagonian Andes. *J. Geol. Soc.* 1011–1022.
- Calderón, M., Hervé, F., Fuentes, F., Fodick, J.C., Sepúlveda, F., Galaz, G., 2016. Tectonic evolution of Paleozoic and Mesozoic andean metamorphic complexes and the Rocas Verdes ophiolites in southern Patagonia. In: Ghiglione, M. (Ed.), *Geodynamic Evolution of the Southernmost Andes: Connections with the Scotia Arc*. Springer Earth System Series. <https://doi.org/10.1007/978-3-319-39727-6>.
- Carley, T.L., Miller, C.F., Wooden, J.L., Bindeman, I.N., Barth, A.P., 2011. Zircon from historic eruptions in Iceland: reconstructing storage and evolution of silicic magmas. *Mineral. Petrol.* 102, 1–27.
- Casquet, C., Rapela, C.W., Pankhurst, R.J., Baldo, E.G., Galindo, C., Fanning, C.M., Dahlquist, J.A., Saavedra, J., 2012. A history of Proterozoic terranes in southern south America: from Rodinia to Gondwana. *Geosci. Front.* 3, 137–145.
- Castillo, P., Fanning, C.M., Pankhurst, R.J., Hervé, F., Rapela, C.W., 2017. Zircon O- and Hf-isotope constraints on the genesis and tectonic significance of Permian magmatism in Patagonia. *J. Geol. Soc.* 174, 803–816.
- Cawood, P.A., 2005. Terra Australis orogen: Rodinia breakup and development of the Pacific and Iapetus margins of Gondwana during the neoproterozoic and Paleozoic. *Earth Sci. Rev.* 69, 249–279.
- Claiborne, L.L., Miller, C.F., Flanagan, D.M., Clyne, M.A., Wooden, J.L., 2010. Zircon reveals protracted magma storage and recycling beneath Mount St. Helens. *Geology* 38, 1011–1014.
- Clemens, J.D., Stevens, G., Mayne, M.J., 2021. Do arc silicic magmas form by fluid-fluxed melting of older arc crust or fractionation of basaltic magmas? *Contrib. Mineral. Petrol.* 176.
- Condie, K.C., Belousova, E., Griffin, W.L., Sircombe, K.N., 2009. Granitoid events in space and time: constraints from igneous and detrital zircon age spectra. *Gondwana Res.* 15, 228–242.
- De La Cruz, R., Suárez, M., 2006. Geología del Área Puerto Guadal–Puerto Sánchez. Región Aisén del General Carlos Ibáñez del Campo, escala, 1(100,000).
- Dube, B., Zubia, M.A., Dunning, G., Villeneuve, M., 2003. Estudio geocronológico de los campos filonianos de baja sulfuración hospedados en la Formación Chon Aike en el Macizo del Deseado, provincial de Santa Cruz. In: Zubia, M., Genini, A. (Eds.), *Yacimientos auroargentíferos epitermales del Macizo del Deseado, Provincia de Santa Cruz*. SEGEMAR Serie Contribuciones Técnicas Recursos Minerales 13/D, pp. 17–24.
- Farina, F., Dini, A., Davies, J.H.F.L., Ovtcharova, M., Greber, N.D., Bouvier, A.-S., Baumgartner, L., Ulyanov, A., Schaltegger, U., 2018. Zircon petrochronology reveals the timescale and mechanism of anatectic magma formation. *Earth Planet Sci. Lett.* 495, 213–223.
- Féraud, G., Alric, V., Fornari, M., Bertrand, H., Haller, M., 1999. 40Ar/39Ar dating of the Jurassic volcanic province of Patagonia: migrating magmatism related to Gondwana break-up and subduction. *Earth Planet Sci. Lett.* 172, 83–96.
- Flowerdew, M.J., Millar, I.L., Vaughan, A.P.M., Horstwood, M.S.A., Fanning, C.M., 2006. The source of granitic gneisses and migmatites in the Antarctic Peninsula: a combined U–Pb SHRIMP and laser ablation Hf study of complex zircons. *Contrib. Mineral. Petrol.* 151, 751–768.
- Foley, M.L., Putlitz, B., Baumgartner, L.P., Ulyanov, A., Siron, G., 2021. Isotope Characteristics of a Large Silicic Province: Crustal versus Mantle Processes in the Generation of the Jurassic Chon Aike Province (Argentina), vol. 53. Geological Society of America Abstracts with Programs, p. 6.
- Forsythe, R., 1982. The late Palaeozoic to early Mesozoic evolution of southern South America: a plate tectonic interpretation. *J. Geol. Soc.* 139, 671–682.
- Fodick, J.C., Grove, M., Hourigan, J.K., Calderón, M., 2013. Retroarc deformation and exhumation near the end of the Andes, southern Patagonia. *Earth Planet Sci. Lett.* 361, 504–517.
- Ghiglione, M.C., Ronda, G., Suárez, R.J., Aramendía, I., Barberón, V., Ramos, M.E., Tobal, J., García Morabito, E., Martinod, J., Sue, C., 2019. Structure and tectonic evolution of the South Patagonian fold and thrust belt: coupling between subduction dynamics, climate, and tectonic deformation. In: Horton, B., Folguera, A. (Eds.), *Andean Tectonics* 24.
- Giacosa, R., Fracchia, D., Heredia, N., 2012a. Structure of the southern Patagonian Andes at 49° S, Argentina. *Geol. Acta* 10, 265–282.
- Giacosa, R., Fracchia, D., Heredia, N., Pereyra, F., 2012b. Hoja Geológica 4972-III y 4975-IV, el Chaltén, provincial de Santa Cruz. *Rev. Asoc. Geol. Argent.* 71, 575–584.

- Glazner, A.F., 2007. Thermal limitations on incorporation of wall rock into magma. *Geology* 35, 319–322.
- González, P.D., Sato, A.M., Naipauer, M., Varela, R., Llambías, E.J., Basei, M., Sato, J., Spösser, W., 2011. Does Patagonia represent a missing piece detached from the Ross Orogen? In: Schmitt, R.S., et al. (Eds.), *Gondwana 14: Reuniting Gondwana: East Meets West*. Rio de Janeiro, Brasil, Abstracts, p. 153.
- González, P.D., Sato, A.M., Naipauer, M., Varela, R., Basei, M., Sato, J., Llambías, E.J., Chemale, F., Dorado, A.C., 2018. Patagonia-Antarctica Early Paleozoic conjugate margins: Cambrian synsedimentary silicic magmatism, U-Pb dating of K-bentonites, and related volcanogenic rocks. *Gondwana Res.* 63, 186–225.
- Guido, D.M., Escayola, M.P., Schalamuk, I.B., 2004. The basement of the Deseado massif at Bahía Laura, Patagonia, Argentina: a proposal for its evolution. *J. S. Am. Earth Sci.* 16, 567–577.
- Guillermin, Z., 2019. Geology and Geochemistry of a Rhyolitic Volcanic Dome: El Chaltén, Patagonia-Argentina. MSc Thesis Université de Lausanne, Institute des Sciences de la Terre, Lausanne, Switzerland, p. 129.
- Gust, D.A., Biddle, K.T., Phelps, D.W., Uliana, M.A., 1985. Associated middle to late Jurassic volcanism and extension in southern south America. *Tectonophysics* 116, 223–253.
- Harrington, H.J., 1962. Paleogeographic development of south America. *AAPG (Am. Assoc. Pet. Geol.) Bull.* 46, 1173–1814.
- Hervé, F., Fanning, C.M., Pankhurst, R.J., 2003. Detrital zircon age patterns and provenance in the metamorphic complexes of southern Chile. *J. S. Am. Earth Sci.* 16, 107–123.
- Hervé, F., Miller, H., Pimpirev, C., 2006. Patagonia-Antarctica connections before Gondwana break-up. In: Fütterer, D.K., Damaske, D., Kleinschmidt, G., Miller, H., Tessensohn, F. (Eds.), *Antarctica*. Springer, Berlin, Heidelberg.
- Hervé, F., Pankhurst, R.J., Fanning, C.M., Calderón, M., Yaxley, G.M., 2007a. The South Patagonian batholith: 150 My of granite magmatism on a plate margin. *Lithos* 97, 373–394.
- Hervé, F., Massonne, H.J., Calderón, M., Theye, T., 2007b. Metamorphic P-T conditions of late Jurassic rhyolites in the Magallanes fold and thrust belt, Patagonian Andes, Chile. *J. Iber. Geol.* 33, 5–16.
- Hervé, F., Calderón, M., Faúndez, V., 2008. The metamorphic complexes of the Patagonian and Fuegian Andes. *Geol. Acta* 6, 43–53.
- Hervé, F., Calderón, M., Fanning, C.M., Kraus, S., Pankhurst, R.J., 2010a. SHRIMP chronology of the Magallanes Basin basement, Tierra del Fuego: Cambrian plutonism and Permian high-grade metamorphism. *Andean Geol.* 37, 253–275.
- Hervé, F., Fanning, C.M., Pankhurst, R.J., Mpodozis, C., Klepeis, K., Calderón, M., Thomson, S.N., 2010b. Detrital zircon SHRIMP U-Pb age study of the Cordillera Darwin Metamorphic Complex of Tierra del Fuego: sedimentary sources and implications for the evolution of the Pacific margin of Gondwana. *J. Geol. Soc. London* 167, 555–568.
- Horstwood, M.S.A., Košler, J., Gehrels, G., Jackson, S.E., McLean, N.M., Paton, C., Pearson, N.J., Sircombe, K., Sylvester, P., Vermeesch, P., Bowring, J.F., Condon, D. J., Schoene, B., 2016. Community-derived standards for LA-ICP-MS U-(Th)-Pb geochronology – uncertainty Propagation, age interpretation and data reporting. *Geostand. Geoanal. Res.* 40, 311–332.
- Jackson, S.E., 2008. Lamtrace data reduction software for LA-ICP-MS. In: Sylvester, P. (Ed.), *Laser Ablation ICP-MS in the Earth Sciences: Current Practices and Outstanding Issues*, Short Course Series, vol. 40. Mineralogical Association of Canada, 305–307.
- Jacob, J.B., Moya, J.F., Fiannacca, P., Laurent, O., Bachmann, O., Janoušek, V., Federico, F., Villaros, A., 2021. Crustal Melting vs. Fractionation of Basaltic Magmas: Part 2, Attempting to Quantify Mantle and Crustal Contributions in Granitoids. *Lithos*, p. 106292.
- Kay, S.M., Ramos, V.A., Márquez, M., 1993. Dominant slab-melt component in Cerro Pampa adakite lavas erupted prior to the collision of the Chile rise in Southern Patagonia. *J. Geol.* 101, 703–714.
- Leanza, A.F., 1972. Andes patagónicas australes. In: Leanza, A.F. (Ed.), *Geología Regional Argentina*. Córdoba, Academia de Ciencias, pp. 689–706.
- Leresche, S., 2013. Etude structurale, géochimique, géochimique, géochronologique et pétrographique d'une partie des roches encaissantes à l'Est de l'intrusion du Mt. Fitz Roy (Patagonie, Argentine). MSc Thesis Université de Lausanne, Institute des Sciences de la Terre, Lausanne Switzerland, p. 111.
- Lopez, R.G., 2006. Estudio Geológico-Metalogénico del área oriental al curso medio del Río Pinturas, sector noroeste del Macizo del Deseado, provincial de Santa Cruz, Argentina. Ph.D. thesis. Universidad de La Plata, p. 206.
- Ludwig, K.R., 2003. User's Manual for Isoplot 3.00: A Geochronological Toolkit for Microsoft, Excel. Kenneth R. Ludwig, Berkeley CA.
- Malkowski, M.A., Grove, M., Graham, S.A., 2016. Unzipping the Patagonian Andes-Long-lived influence of rifting history on foreland basin evolution. *Lithosphere* 8, 23–28.
- Millar, I.L., Pankhurst, R.J., Fanning, C.M., 2002. Basement chronology of the Antarctic Peninsula: recurrent magmatism and anatexis in the Palaeozoic Gondwanan margin. *J. Geol. Soc.* 159, 145–157.
- Miller, C.F., Watson, E.B., Harrison, T.M., 1988. Perspectives on the source, segregation and transport of granitoid magmas. *Trans. R. Soc. Edinb. Earth Sci.* 79, 135–156.
- Miller, C.F., Hanchar, J.M., Wooden, J.L., Bennett, V.C., Harrison, T.M., Wark, D.A., Foster, D.A., 1992. Source region of a granite batholith: evidence from lower crustal xenoliths and inherited accessory minerals. *Trans. R. Soc. Edinb. Earth Sci.* 83, 49–62.
- Miller, C.F., McDowell, S.M., Mapes, R.W., 2003. Hot and cold granites? Implication of zircon saturation temperatures and preservation of inheritance. *Geology* 31, 529–532.
- Miller, J.S., Matzel, J.E.P., Miller, C.F., Burgess, S.D., Miller, R.B., 2007. Zircon growth and recycling during the assembly of large, composite arc plutons. *J. Volcanol. Geoth. Res.* 167, 282–299.
- Miller, C.F., Furbish, D.J., Walker, B.A., Claiborne, L.L., Koteas, G.C., Bleick, H.A., Miller, J.S., 2011. Growth of plutons by incremental emplacement of sheets in crystal-rich host: evidence from Miocene intrusions of the Colorado River region, Nevada, USA. *Tectonophysics* 500, 65–77.
- Moreira, P., González, P., Fernández, R., Echeveste, H., Schalamuk, I., Etcheverry, R., 2005. El basamento de bajo grado de las Estancias La Modesta y La Josefina, Macizo del Deseado, Provincia de Santa Cruz. *Rev. Asoc. Geol. Argent.* 60, 49–63.
- Moreira, P., Echeveste, H., Fernández, R., Hartmann, L.A., Santos, J.O.S., Schalamuk, I., 2009. Dispositional age of Jurassic epithermal gold-silver ore in the Deseado massif, Patagonia, Argentina, based on Manantial Espejo and La Josefina prospects. *N. Jb. Geol. Paläont. Abh.* 253, 25–40.
- Moreira, P., Fernández, R., Hervé, F., Fanning, C.M., Schalamuk, I.A., 2013. Detrital zircons U-Pb SHRIMP ages and provenance of La Modesta formation, Patagonia Argentina. *J. S. Am. Earth Sci.* 47, 32–46.
- Muller, V.A.P., Calderón, M., Fosdick, J.C., Ghiglione, M.C., Cury, L.F., Massonne, H.-J., Fanning, C.M., Warren, C.J., Ramírez de Arellano, C., Sternai, P., 2021. The closure of the Rocas Verdes basin and early tectono-metamorphic evolution of the Magallanes fold-and-thrust belt, southern Patagonian Andes (52–54°S). *Tectonophysics* 789.
- Müntener, O., Ewing, T., Baumgartner, L.P., Manzini, M., Roux, T., Pellaud, P., Allemann, L., 2018. Source and fractionation controls on subduction-related plutons and dike swarms in southern Patagonia (Torres del Paine area) and the low Nb/Ta of upper crustal igneous rocks. *Contrib. Mineral. Petrol.* 173, 38.
- Navarrete, C., Gianni, G., Encinas, A., Márquez, M., Kamerbeek, Y., Valle, M., Folguera, A., 2019. Triassic to Middle Jurassic geodynamic evolution of southwestern Gondwana: from a large flat-slab to mantle plume suction in a rollback subduction setting. *Earth Sci. Rev.* 194, 125–159.
- Navarrete, C., Butler, K.L., Hurley, M., Márquez, M., 2020. An early Jurassic graben caldera of Chon Aike silicic LIP at the southernmost massif of the world: the Deseado caldera, Patagonia, Argentina. *J. S. Am. Earth Sci.* 101, 102626.
- Nescher, P., 2013. Petrography, structural geology. MSc Thesis. In: *Geochemistry and Metamorphism of the Rocks in the Eastern Fitz Roy Foothills in Patagonia, Argentina*, vol. 155. Université de Lausanne, Institute des Sciences de la Terre, Lausanne Switzerland.
- Orihashi, Y., Anma, R., Motoki, A., Haller, M.J., Hirata, D., Iwano, H., Sumino, H., Ramos, V.A., 2013. Evolution history of the crust underlying Cerro Pampa, Argentine Patagonia: constraint from LA-ICP-MS U-Pb ages for exotic zircons in the Mid-Miocene adakite. *Geochem. J.* 47, 235–247.
- Pankhurst, R.J., Rapela, C.R., 1995. Production of Jurassic rhyolite by anatexis of the lower crust of Patagonia. *Earth Planet Sci. Lett.* 134, 23–26.
- Pankhurst, R.J., Leat, P.T., Sruoga, P., Rapela, C.W., Márquez, M., Storey, B.C., Riley, T. R., 1998. The Chon Aike silicic igneous province of Patagonia and related rocks in Antarctica: a silicic large igneous province. *J. Volcanol. Geoth. Res.* 81, 113–136.
- Pankhurst, R.J., Riley, T.R., Fanning, C.M., Kelley, S.P., 2000. Episodic silicic volcanism in Patagonia and the Antarctic Peninsula: chronology of magmatism associated with the break-up of Gondwana. *J. Petrol.* 41, 603–625.
- Pankhurst, R.J., Rapela, C.W., Loske, W.P., Márquez, M., Fanning, C.M., 2003. Chronological study of the pre-Permian basement rocks of southern Patagonia. *J. S. Am. Earth Sci.* 16, 27–44.
- Pankhurst, R.J., Rapela, C.W., Fanning, C.M., Márquez, M., 2006. Gondwanide continental collision and the origin of Patagonia. *Earth Sci. Rev.* 76, 235–257.
- Pankhurst, R.J., Rapela, C.W., López De Luchi, M.G., Rapalini, A.E., Fanning, C.M., Galindo, C., 2014. The Gondwana connections of northern Patagonia. *J. Geol. Soc. London* 171, 313–328.
- Pavón Pivetta, C., Gregori, D., Benedini, L., Garrido, M., Strazzere, L., Gerales, M., Costa dos Santos, A., Marcos, P., 2019. Contrasting tectonic settings in Northern Chon Aike Igneous Province of Patagonia: subduction and mantle plume-related volcanism in the Marifil formation. *Int. Geol. Rev.* <https://doi.org/10.1080/00206814.2019.1669227>.
- Permy-Vidal, C., Moreira, P., Guido, D.M., Fanning, C.M., 2014. Linkages between the southern Patagonia Pre-Permian basements: new insights from detrital zircons U-Pb SHRIMP ages from the Cerro Negro District. *Geol. Acta* 12, 137–150.
- Permy-Vidal, C., Guido, D.M., Shatwell, D., Lopez, S.M., Páez, G.N., Moreira, P., 2021. The Cerro Negro epithermal district, northwestern Deseado Massif (Patagonia, Argentina): new insights from telescoped volcanic-hydrothermal systems. *J. S. Am. Earth Sci.* 105, 103017.
- Pezzuchi, H., 1978. Estudio geológico de la zona de Estancia Dos Hermanos-Estancia 25 de Marzo y adyacentes, departamento Deseado, Provincia de Santa Cruz. Unpublished PhD thesis. Universidad Nacional de La Plata, Argentina.
- Poblete, J.A., Bissig, T., Mortensen, J.K., Gabites, J., Friedman, R., Rodriguez, M., 2013. The Cerro Bayo district, Chilean Patagonia: late Jurassic to cretaceous magmatism and protracted history of epithermal Ag-Au Mineralization. *Econ. Geol.* 109, 487–502.
- Ramírez de Arellano, C., Putlitz, B., Müntener, O., Ovtcharova, M., 2012. High precision U/Pb zircon dating of the Chaltén plutonic complex (Cerro Fitz Roy, Patagonia) and its relationship to arc migration in the southernmost Andes. *Tectonics* 31.
- Ramos, V.A., 1989. Andean Foothills structures in northern Magallanes Basin, Argentina. *Am. Assoc. Petrol. Geol. Bull.* 73, 887–903.
- Ramos, V.A., 2008. Patagonia: a Paleozoic continent adrift? *J. S. Am. Earth Sci.* 26, 235–251.
- Ramos, V.A., 2010. The Grenville-age basement of the Andes. *J. S. Am. Earth Sci.* 29, 77–91.

- Ramos, V.A., Naipauer, M., 2014. Patagonia: where does it come from? *J. Iber. Geol.* 40, 367–379.
- Rapela, C.W., Pankhurst, R., 1992. The granites of northern Patagonia and the gastre fault system in relation to the break-up of Gondwana. In: Storey, B., Alabaster, T., Pankhurst, R. (Eds.), *Magmatism and the Causes of Continental Break-Up*, vol. 68. Geological Society Special Publications, pp. 209–220.
- Rapela, C.W., Pankhurst, R.J., 1996. Monzonite suites: the innermost cordilleran plutonism of Patagonia. *Trans. R. Soc. Edinb. Earth Sci.* 87, 193–203.
- Rapela, C.W., Pankhurst, R.J., Fanning, C.M., Hervé, F., 2005. In: P. M. Leat, P.T., Pankhurst, R.J. (Eds.), *Pacific Subduction Coeval with the Karoo Mantle Plume: the Early Jurassic Subcordilleran Belt of Northwestern Patagonia*. From Vaughan, Terrane Processes at the Margins of Gondwana, vol. 246. Geological Society, London, Special Publications, pp. 217–239.
- Rapela, C.W., Pankhurst, R.J., Casquet, C., Dahlquist, J.A., Fanning, C.M., Baldo, E.G., Galindo, C., Alasino, P.H., Ramacciotti, C.D., Verdecchia, S.O., Murra, J.A., Basei, M.A.S., 2018. A review of the Famatinian Ordovician magmatism in southern South America: evidence of lithosphere reworking and continental subduction in the early proto-Andean margin of Gondwana. *Earth Sci. Rev.* 187, 259–285.
- Riccardi, A., 1971. Estratigrafía en el oriente de la Bahía de la Lancha, Lago San Martín, Santa Cruz, Argentina. *Revista Museo de la Plata, nueva serie* 61 (7), 245–318.
- Riley, T.R., Leat, P., 1999. Large volume silicic volcanism along the proto-Pacific margin of Gondwana: lithological and stratigraphical investigations from the Antarctic Peninsula. *Geol. Mag.* 136, 1–16.
- Riley, T.R., Leat, P.T., Pankhurst, R.J., Harris, C., 2001. Origins of large volume rhyolitic volcanism in the Antarctic Peninsula and Patagonia by crustal melting. *J. Petrol.* 42, 1043–1065.
- Riley, T.R., Flowerdew, M.J., Whitehouse, M.J., 2012. U-Pb ion-microprobe zircon geochronology from the basement inliers of eastern Graham Land, Antarctic Peninsula. *J. Geol. Soc.* 169, 381–393. London.
- Riley, T.R., Flowerdew, M.J., Pankhurst, R.J., Curtis, M.L., Millar, I.L., Fanning, C.M., Whitehouse, M.J., 2016. Early Jurassic magmatism on the Antarctic Peninsula and potential correlation with the subcordilleran plutonic belt of Patagonia. *J. Geol. Soc.* 174, 365–376.
- Riley, T.R., Flowerdew, M.J., Millar, I.L., Whitehouse, M.J., 2020. Triassic magmatism and metamorphism in the Antarctic Peninsula: identifying the extent and time of the Peninsula orogeny. *J. S. Am. Earth Sci.* 103, 102732.
- Rojo, D., Calderón, M., Ghiglione, M.C., Suárez, R.J., Quezada, P., Cataldo, J., Hervé, F., Charrier, R., Galaz, G., Suárez, M., Guettner, G., Babinski, M., 2021a. The low-grade basement at Península La Carmela, Chilean Patagonia: new data for unraveling the pre-Permian basin nature of the Eastern Andean Metamorphic Complex. *Int. J. Earth Sci.* 110, 2021–2042.
- Rojo, D., Calderón, M., Hervé, F., Díaz, J., Suárez, R., Ghiglione, M.C., Fuentes, F., Theye, T., Cataldo, J., Sandoval, D., Viehhaus, T., 2021b. Petrology and tectonic evolution of late Paleozoic mafic-ultramafic sequences and the Leones Pluton of the eastern andean metamorphic complex (46–47°S), southern Chile. *J. S. Am. Earth Sci.* 108, 103198.
- Rolando, A.P., Hartmann, L.A., Santos, J.O.S., Fernandez, R.R., Etcheverry, R.O., Schalamuk, I.A., McNaughton, N.J., 2002. SHRIMP zircon U-Pb evidence for extended Mesozoic magmatism in the Patagonian Batholith and assimilation of Archean crustal components. *J. S. Am. Earth Sci.* 15, 267–283.
- Rolando, A.P., Hartmann, L.A., Santos, J.O., Fernandes, R.R., Etcheverry, R.O., Schalamuk, I.A., McNaughton, N.J., 2004. SHRIMP U-Pb zircon dates from igneous rocks from the Fontana Lake region, Patagonia: implications for the age of magmatism, Mesozoic geological evolution and age of basement. *Rev. Assoc. Geol. Argent.* 59, 671–684.
- Schilling, M.E., Carlson, R.W., Tassara, A., Conceição, R.V., Bertotto, G.W., Vásquez, M., Muñoz, D., Jalowitzki, T., Gervasoni, F., 2017. The origin of Patagonia revealed by Re-Os systematics of mantle xenoliths. *Precambrian Res.* 294, 15–32.
- Schwartz, J.J., Gromet, L.P., Miró, R., 2008. Timing and duration of the calc-alkaline arc of the Pampean orogeny: implications for the late neoproterozoic to Cambrian evolution of western Gondwana. *J. Geol.* 116, 39–61.
- Seitz, S., Putlitz, B., Baumgartner, L.P., Bouvier, A.-S., 2018. The role of crustal melting in the formation of rhyolites: constraints from SIMS oxygen isotope data (Chon Aike Province, Patagonia, Argentina). *Am. Mineral.* 103, 2011–2027.
- Sepúlveda, F.A., Palma-Heldt, S., Hervé, F., Fanning, C.M., 2010. Permian depositional age of metaturbidites of the Duque of York Complex, southern Chile: U-Pb SHRIMP data and palynology. *Andean Geol.* 37, 375–397.
- Sláma, J., Košler, J., Condon, D.J., Crowley, J.L., Gerdes, A., Hanchar, J.M., Horstwood, M.S.A., Morris, G.A., Nasdala, L., Norberg, N., Schaltegger, U., Schoene, B., Tubrett, M.N., Whitehouse, M.J., 2008. Plešovice zircon — a new natural reference material for U–Pb and Hf isotopic microanalysis. *Chem. Geol.* 249, 1–35.
- Söllner, F., Miller, H., Hervé, M., 2000. An Early Cambrian granodiorite age from the pre-Andean basement of Tierra del Fuego (Chile): the missing link between South America and Antarctica? *J. S. Am. Earth Sci.* 13, 163–177.
- Suárez, R., González, P.D., Ghiglione, M.C., 2019a. A review on the tectonic evolution of the Paleozoic-Triassic basins from Patagonia: record of protracted westward migration of the pre-Jurassic subduction zone. *J. S. Am. Earth Sci.* 95, 102256.
- Suárez, R., Ghiglione, M.C., Calderón, M., Sue, C., Martinod, J., Guillaume, B., Rojo, D., 2019b. The metamorphic rocks of the Nunatak Viedma in the southern Patagonian Andes: provenance source and implications for the early Mesozoic Patagonia–Antarctic Peninsula connection. *J. S. Am. Earth Sci.* 90, 471–486.
- Varela, R., Basei, M.A.S., Cingolani, C.A., Siga Jr., O., Passarelli, C.R., 2005. El basamento cristalino de los Andes norpatagónicos en Argentina: geocronología e interpretación tectónica. *Rev. Geol. Chile* 32, 167–187.
- Weinberg, R.F., Becchio, R., Farias, P., Suzaño, N., Sola, A., 2018. Early Paleozoic accretionary orogenies in NW Argentina: growth of West Gondwana. *Earth Sci. Rev.* 187, 219–247.
- Widmann, P., Davies, J.H.F.L., Schaltegger, U., 2019. Calibrating chemical abrasion: its effects on zircon crystal structure, chemical composition and U-Pb age. *Chem. Geol.* 511, 1–10.
- Zaffarana, C.B., Somoza, R., López de Luchi, M., 2014. The late Triassic Central Patagonian batholith: magma hybridization 40Ar/39Ar ages and thermobarometry. *J. S. Am. Earth Sci.* 55, 94–122.